

# **Spectroscopic investigation into papain conformational changes in the presence of an anionic surfactant**

**A Dissertation**

Submitted for the partial fulfilment of the Degree

of

**Master of Science**

**In**

**Chemistry**

By

**Nitika Aggarwal**

(Registration No.: 302102013)

*Under the guidance of*

**Dr. Mily Bhattacharya**

(Assistant Professor)



**THAPAR INSTITUTE**  
OF ENGINEERING & TECHNOLOGY  
(Deemed to be University)

**School of Chemistry and Biochemistry**

**Thapar Institute of Engineering and Technology**

**Patiala- 147004, Punjab**

## CANDIDATE'S DECLARATION

I, hereby, declare that the work being presented in the dissertation entitled "**Spectroscopic investigation into papain conformational changes in the presence of an anionic surfactant**" in partial fulfilment of the requirement for the award of the degree of **Masters of Science in Chemistry** and being submitted to School of Chemistry and Biochemistry, Thapar Institute of Engineering and Technology, Patiala is my own research work carried out during the period of January to July 2023 under the supervision of **Dr. Mily Bhattacharya**. I have not submitted the contents embodied in this dissertation for the award of any degree elsewhere.



Nitika Aggarwal

Date: 20 July 2023

It is certified that the above statement made by the student is correct to the best of my knowledge and belief.



Dr. Mily Bhattacharya

Assistant Professor

School of Chemistry and Biochemistry

Thapar Institute of Engineering and Technology, Patiala- 147004

## CERTIFICATE

This is to certify that the dissertation entitled "**Spectroscopic investigation into papain conformational changes in the presence of an anionic surfactant**", being submitted by **Ms. Nitika Aggarwal** in the partial fulfilment of requirement for the award of the degree of **Masters of Science in Chemistry** and being submitted to the School of Chemistry and Biochemistry, Thapar Institute of Engineering and Technology, Patiala is a bonafide work carried out by her under my supervision. The work has reached the standard necessary for submission, and the contents of this dissertation have not been submitted to any other university or institute for the award of any degree or diploma.



Dr. Mily Bhattacharya

Assistant Professor

School of Chemistry and Biochemistry

Thapar Institute of Engineering and Technology, Patiala- 147004

## ACKNOWLEDGEMENT

I would like to express my profound gratitude to my supervisor, **Dr. Mily Bhattacharya**, Assitant Professor, School of Chemistry and Biochemistry, Thapar Institute of Engineering and Technology, Patiala. Her guidance and advice carried me through all the stages of my project. I will be always thankful to her for directing the right path. It was a great privilege and honor to work and study under her guidance.

I am indebted to **Prof. Satnam Singh**, Head of School of Chemistry and Biochemistry for their support in completing this endeavor. I would like to give special thanks to **Prof. Samrat Mukhopadhyay's laboratory** (IISER Mohali) for allowing me to use the CD spectroscopy, fluorescence anisotropy, Zeta Poetential measurements and TEM.

I sincerely appreciate the contribution of research scholars of my lab, Ms. Anjali Giri, Ms. Jaspreet Kaur, Ms. Deepika and Ms. Mandeep Kaur for their enthusiastic participation and contributions. I would especially like to express my gratitude towards my mentor, **Ms. Anjali Giri** for being my support from the start and giving me the confidence in my work via her invaluable efforts. I will remember the kindness, support and advice of **Ms. Jaspreet Kaur** and **Ms. Deepika** that showed to me and their assistance with my experiments. I sincerely admire the contribution of **Ms. Mandeep Kaur** for her supportive and helping nature.

I would like to extend my thanks to SCBC staff and lab technicians for their cooperation during the pursuit of the programme. I am very grateful to all my classmates and friends.

Last but not the least, I would like to express my greatest gratitude towards my parents for their support and motivation.

Date: 20 July 2023



Signature of Candidate

Nitika Aggarwal

Full Name of Candidate

## **ABSTRACT**

Globular proteins contain substantial numbers of  $\alpha$ - helices and  $\beta$ - sheets folded into a compact structure that is stabilized by both polar and non- polar interactions. The diversity of protein structures reflect the remarkable variety of functions performed by globular proteins: binding, catalysis, regulations etc. The hydrophobic part of amino acids side chains are buried, closely packed, in the interior of a globular protein while the hydrophilic amino acids of the side chains lie on the surface of the globular proteins and are usually exposed to the water. The most prominent form of protein aggregation is associated with a wide range of human disorders. The globular protein, Papain, is a proteolytic enzyme, obtained from the latex of *Carica papaya*. It is well studied due to it's wide application in cosmetics, food industries and also has many medicinal applications. We have studied the aggregation of papain in the presence of sodium dodecyl sulfate (SDS) at pH 7.4 at room temperature with the help of different spectroscopic and microscopic techniques such as steady- state fluorescence using different extrinsic and intrinsic fluorophores, Circular Dichroism (CD), Field- Emission Scanning Electron Microscopy (FESEM) and Transmission Electron Microscopy (TEM). We have observed that aggregates were formed at higher concentrations of SDS and papain. The results have shown that  $\beta$ - sheets are formed at an expense of  $\alpha$ - helices during aggregation at higher concentrations of SDS. Morphological studies reveals that the aggregates formed amorphous in nature, not fibrillar.

## TABLE OF CONTENTS

S.NO.	CONTENTS	PAGE NO.
	<b>DECLARATION</b>	
	<b>CERTIFICATE</b>	
	<b>ACKNOWLEDGEMENT</b>	
	<b>ABSTRACT</b>	
	<b>TABLE OF CONTENTS</b>	
	<b>LIST OF TABLES</b>	
	<b>LIST OF FIGURES</b>	
<b>CHAPTER 1</b>	<b>INTRODUCTION</b>	<b>1-7</b>
<b>CHAPTER 2</b>	<b>LITERATURE REVIEW</b>	<b>8-13</b>
<b>CHAPTER 3</b>	<b>MATERIALS AND METHODS</b>	<b>14-18</b>
3.1	Reagents used	14
3.2	Glassware and Labware used	14
3.3	Methodologies	14-18
	3.3.1    Analysis of Sequence Statistics	14
	3.3.2    Stock Solutions Preparation	14-15
	3.3.3    Steady- state fluorescence experiment	15-17
	3.3.4    Circular Dichroism measurements	17
	3.3.5    Zeta Potential measurements	17-18

	3.3.6	Field Emission Scanning Electron Microscopy (FESEM)	18
	3.3.7	Transmission Electron Microscopy (TEM):	18
<b>CHAPTER 4:</b>	<b>RESULTS AND DISCUSSION</b>		<b>19-32</b>
	<b>Conclusions</b>		<b>33</b>
	<b>References</b>		<b>34-36</b>
	<b>Plagiarism Report</b>		<b>37</b>

## **LIST OF TABLES**

<b>Table No.</b>	<b>Title</b>	<b>Page No.</b>
<b>TABLE 2.1</b>	Number of amino acid residues in papain	8

## LIST OF FIGURES

<b>Figure no.</b>	<b>Title</b>	<b>Page no.</b>
<b>1.1</b>	Protein secondary structural elements. Adapted from Portland Press, 2020, 64, Stollar E.J.; Smith D.P. Uncovering protein structure, 649-680	2
<b>1.2</b>	(A) shows the formation of unfolded state to native state (B) Thermodynamics of protein folding. Adapted from Portland Press, 2020, 64, Stollar, E.J.; Smith, D.P. Uncovering protein structure, 649- 680.	4
<b>1.3</b>	Formation of amyloids, above and below the pI. Adaped from Khan J.M.; Khan R.H. SDS can be utilized as an Amyloid Inducer: A case study on diverse proteins. PLoS ONE <b>2012</b> , 7.	7
<b>2.1</b>	Representation of primary sequence of papain sequence.	9
<b>2.3</b>	Ribbon diagram of papain (PDB: 1BQI) Pink colour shows the tryptophan amino acis residue present in papain and yellow colour shows the disulfide bonds in papain.	10
<b>2.4</b>	Schematic representation of temperature-induced changes in papain conformation in the absence and presence of SDS. Adapted from Qadeer A.; Zaman M.; Khan R.H. The inhibitory effect of Post- Micellar SDS concentration on Thermal Aggregation and Activity of Papain. Biochemistry (Moscow) <b>2014</b> , 79, 785- 796.	12
<b>4.1</b>	Bioinformatic tools representing the disorderedness using (a) PONDR; (b) charge distribution w.r.t Blob index using NCPR; (c) AGGRESCAN analysis representing hotspot areas.	19
<b>4.2</b>	(a) ThT fluorescence kinetics monitored at 480 nm at 5 $\mu$ M papain, in absence and presence of variable SDS concentration. (b) and (c) shows the ThT fluorescence spectra at 0 min and 70 min in the absence and presence of variable SDS concentration. (d) shows the combined plot of ThT fluorescence spectra at 0 min and 70 min.	20
<b>4.3</b>	(a) ThT fluorescence kinetics monitored at 480	22

	nm in absence and presence of 1 mM SDS, for variable papain concentration. (b) and (c) shows the ThT fluorescence spectra at 0 min and 70 min in presence of 1 mM SDS and variable protein concentration. (d) shows the combined plot at 0 min and 70 min.	
<b>4.4</b>	(a) Tryptophan fluorescence kinetics monitored at 335 nm, at 5 $\mu$ M papain, in absence and presence of variable SDS concentration. (b) and (c) shows the tryptophan fluorescence spectra at 0 min and 70 min in the absence and presence of variable SDS concentration. (d) shows the combined plot at 0 min and 70 min	23
<b>4.5</b>	(a) Tryptophan fluorescence intensity at 335 nm as a function of time in absence and presence of 1 mM SDS, at varied papain concentration. (b) and (c) shows the tryptophan fluorescence emission at 0 min and 70 min presence of 1 mM SDS and varied protein concentration. (d) shows the combined plot at 0 min and 70 min.	24
<b>4.6</b>	a) ANS fluorescence kinetics monitored at 475 nm at 5 $\mu$ M papain, in absence and presence of variable SDS concentration. (b) and (c) shows the ANS fluorescence spectra at 0 min and 70 min in the absence and presence of variable SDS concentration. (d) shows the combined plot of ANS fluorescence spectra at 0 min and 70 min.	25
<b>4.7</b>	(a) ANS fluorescence intensity at 475 nm as a function of time in absence and presence of 1 mM SDS, at varied papain concentration. (b) and (c) shows ANS fluorescence emission at 0 min and 70 min in the presence of 1 mM SDS, at varied protein concentration. (d) shows the combined plot at 0 min and 70 min.	26
<b>4.8</b>	Zeta potential measurements at 5 $\mu$ M papain, in absence and presence of variable SDS concentration.	27
<b>4.9</b>	Far UV-CD Spectra as a function of time at 5 $\mu$ M papain, in the absence and presence of varied SDS concentration. (a), (b),(c),(d) and (e) graphs shows the 200 $\mu$ M, 300 $\mu$ M, 500 $\mu$ M, 1 mM and 2 mM SDS concentrations.	28
<b>4.10</b>	Tryptophan fluorescence anisotropy monitored at 335 nm at 5 $\mu$ M papain, in absence and presence of variable SDS concentration.	30
<b>4.11</b>	Tryptophan fluorescence anisotropy monitored at 335 nm in absence and presence of 1 mM	30

	SDS, for variable papain concentration.	
<b>4.12</b>	Field Emission- Scanning Electron Microscopy images representing the morphology of aggregates; (Scale: 500 nm). (a) papain [5 $\mu$ M] and SDS [300 $\mu$ M], (b) papain [5 $\mu$ M] and SDS [1 mM] , (c) papain [5 $\mu$ M] and SDS [2 mM], (d) papain [50 $\mu$ M] and SDS [1 mM].	31
<b>4.13</b>	Transmission Electron Microscopy images representing the morphology of aggregates; (Scale: 500 nm). (a) papain [5 $\mu$ M] and SDS [1 mM] ,(b) papain [50 $\mu$ M] and SDS [1 mM].	32

# CHAPTER 1

## INTRODUCTION

One of the most crucial kinds of molecules for life and the cornerstone of biochemistry are proteins. Proteins are polymers of ten hundreds of amino acids connected together by peptide bonds whereas peptides are shorter polypeptides (less than 30 amino acids). The side chains and backbone groups interact with one another through a variety of weak interactions, such as vanderwaal's, hydrogen bonds, electrostatic interactions as well as hydrophobic effect, to produce the shape and target interactions of proteins after the amino acids are joined together to form a polypeptide chain. The fact that there are 20 different amino acids and they can be combined in any order leads to an enormous number of conceivable linear combinations and the evolution of tens of thousands of unique proteins and peptides by organisms. Proteins typically donot exist as extended chains; instead, they fold in themselves to create a specific shape through various interactions with their side chains and backbones. Every form has a manner of connecting with other molecules to move and carry out its duties. Proteins are incredibly adaptable due to their variety of forms, sometimes acting as enzymes to catalyze chemical reactions. Since proteins mediate nearly every vital life function, any alterations to their structure as a result of injury, mutation or modification provides a molecular explanation for the disease's origin.<sup>1</sup> There are four levels of description for protein structure. The fundamental structure of a polypeptide refers to how the amino acids are arranged in the chain. Protein structure arranges itself as a result of regular hydrogen bonds forming between the NH groups each peptide bond and its backbone C=O.  $\alpha$ -Helix and  $\beta$ -sheets are two different types of secondary structure.  $\alpha$ -Helix is a right handed coil in which the backbone NH group forms a hydrogen bond with the backbone C=O group of an amino acid that is positioned four residues earlier along the protein sequence.  $\beta$ - Sheets are made up of a pair of or more parallel extended polypeptide chains, or  $\beta$ - strands. Both parallel and antiparallel arrangements are possible. Chains are run either in a single direction to create a parallel  $\beta$ -sheet or in a opposite direction to create an antiparallel  $\beta$ - sheet. Each residue's side chains face away from the sheets and alternately point in different orientations. The interactions between the side chains (R groups) and the way the secondary structure fits together to fold the protein to give overall three dimensional look or tertiary structure; fig. 1.1. The interactions and arrangements of numerous folded protein chains (called subunits).<sup>1</sup>

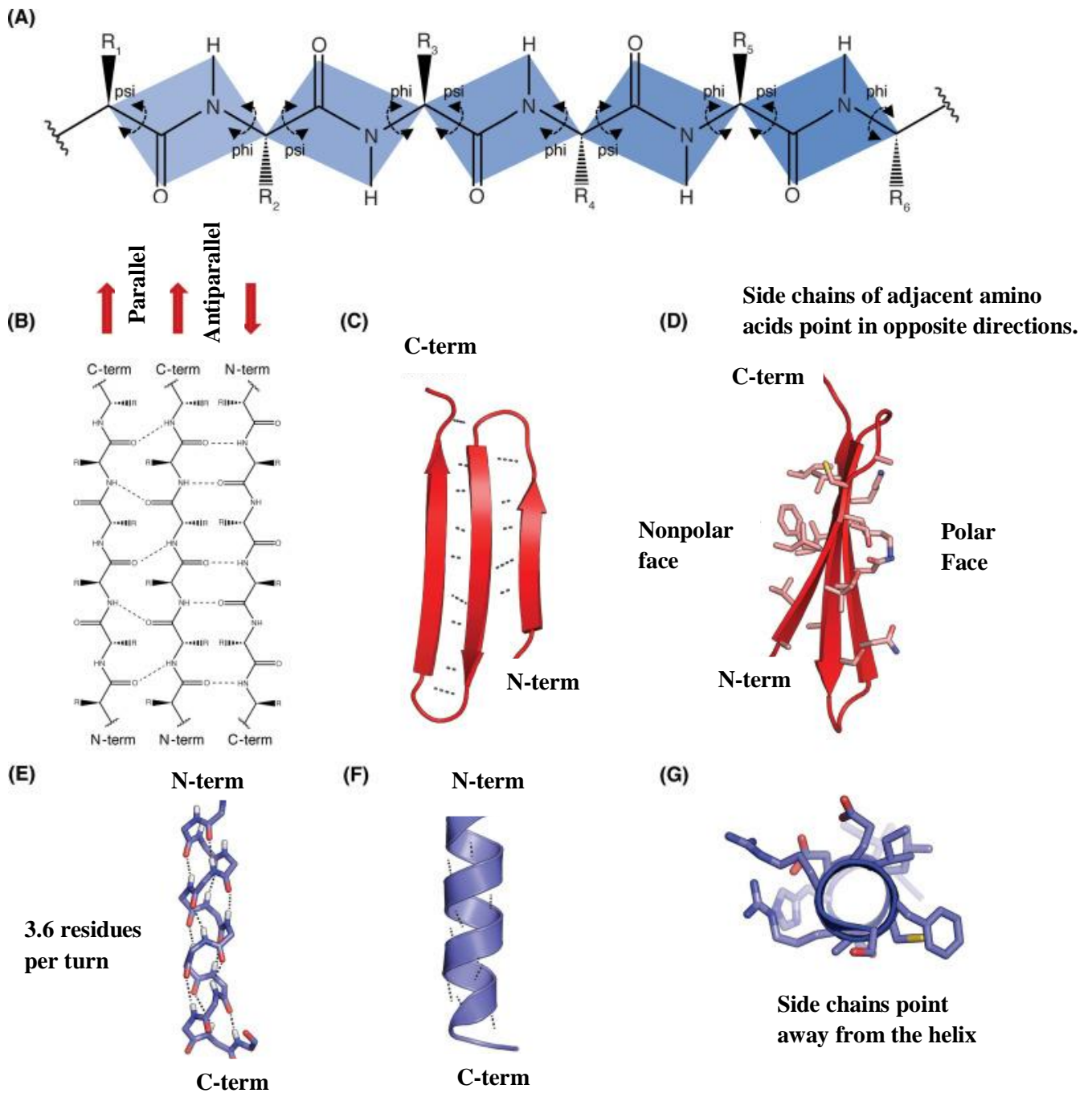


**Figure 1.1:** Protein secondary structural elements (A) Schematic representation of a typical polypeptide molecule. Residue side chains are denoted as R. Symbols denote the flexible chemical bonds that can rotate along the N-C $\alpha$  axis, commonly referred to as phi, and the C $\alpha$ -C axis, also known as psi. (B) shows formation of hydrogen bonds formed in  $\beta$ -strands in parallel and antiparallel  $\beta$ -sheets. (C) shows Cartoon representation (ribbon diagram) shows the antiparallel  $\beta$ -sheets. (D) shows side view of same  $\beta$ -sheet showing the polar and non polar residues sidechains. (E) shows formation of  $\alpha$ -helix from the backbone NH group forms a hydrogen bond with the backbone C=O group of an amino acid that is positioned four residues earlier along the protein sequence. (F) shows the ribbon diagram of  $\alpha$ -helix. (G) shows rotated view of  $\alpha$ -helix. Adapted from Portland Press, 2020, 64, Stollar, E.J.; Smith, D.P. Uncovering protein structure, 649- 680.

Proteins are commonly classified into two types: “folded” proteins (FPs) and “intrinsically unfolded” or “intrinsically disordered” proteins. Many folded proteins, particularly those with a high free energy of unfolding, are in reality so stable that they only survive in the completely folded state until subjected to extremely strong denaturing conditions. FPs are “just” certain instances of stable proteins where the balance leans so heavily towards the folded species that the unfolded form is almost nonexistent. IDPs, on the other hand, are proteins that are so unstable that it is impossible to see the folded form. Due to this, we propose that proteins form a continuous spectrum of folds, with fully folded and entirely unstructured proteins serving as the extreme examples.<sup>2</sup> Figure 1.2 shows the free energy of the native and denatured ensembles of a protein in an environment that favours the native state. This is due to the fact that the native state exhibits a lower free energy compared to the unfolded state. It is important to understand the thermodynamics of protein folding and stability in order to gain insights into their biological functions. The thermodynamic quantity,  $\Delta G$ , which represents the difference in free energy between two states, serves as an indicator of the protein's stability. The ensemble of transition states comprises of partially folded and transient conformations that are not directly observed by experiments. However, these states are crucial for the folding process as they determine the activation barrier for both folding ( $\Delta G^\ddagger$  folding) and unfolding ( $\Delta G^\ddagger$  unfolding).<sup>1</sup> Proteins can be entirely unfolded using chemical denaturants. It has long been understood that proteins often unfold at temperature greater than body temperature of the organism in which they originated.<sup>3</sup> Depending on how you begin the process, the protein folding problem can appear very differently physically for any given protein. We have to make assumptions as to what unfolded conformations are available for a specific protein under various circumstances since protein folding, in which all folding routes and the final folded structure are predicted by basic sequence.<sup>3</sup> Since folding occurs naturally and biological function is primarily related to the folded structure, it may not seem as though the protein folding. However, protein folding or unfolding frequently plays a crucial role in other biocellular activities, including translocation and destruction. Serious problems, illness and even death can result from folding errors. It may seem simpler to study a protein's folding mechanism when its structure is known, but this does not make it any less difficult to do.<sup>4</sup>

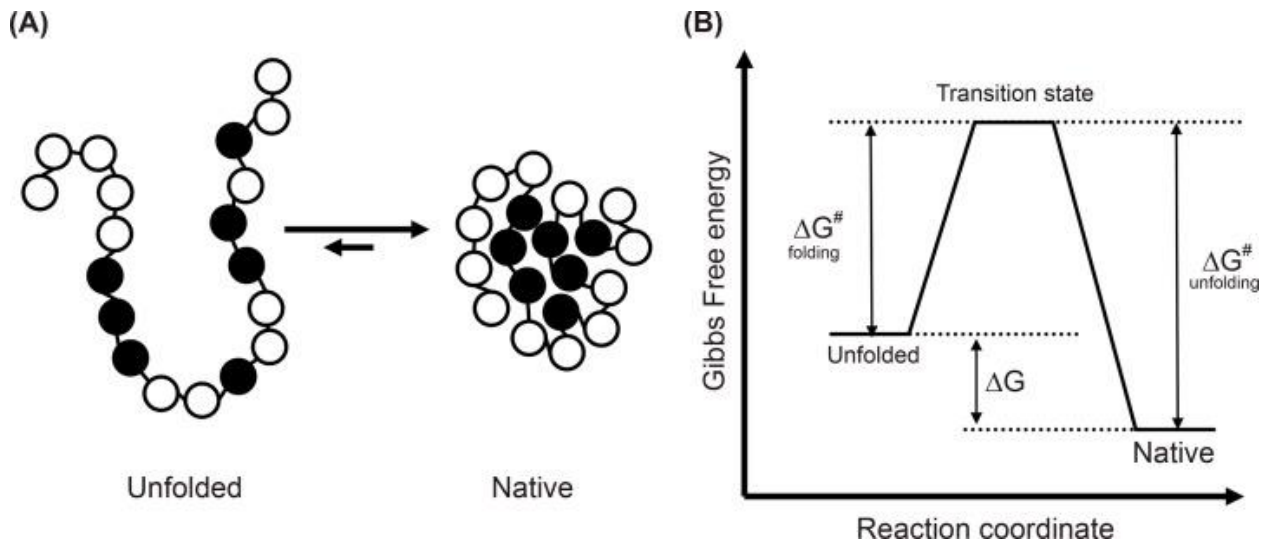


**Figure 1.2:** (A) shows the formation of unfolded state to native state (B) Thermodynamics of protein folding. Adapted from Portland Press, 2020, 64, Stollar, E.J.; Smith, D.P. Uncovering protein structure, 649- 680.

Animals, plants, microbes, yeasts, and viruses all frequently aggregate proteins into highly organized amyloid fibrils or amorphous aggregates, which may or may not be disease-causing or functional. Aggregation, which is mostly caused by misfolding or unfolding, depends on the stability and folding of proteins. The most prominent form of protein aggregation, amyloid fibrils, is associated with a wide range of human disorders.<sup>5</sup> A rapidly expanding area of study is protein aggregation, which is motivated by the pressing need to understand the mechanism underlying neurodegenerative disorders. Protein(s) in their unfolded state(s) come together in a process known as protein aggregation. Precursors of protein aggregation are the folding and unfolding of proteins.<sup>7</sup> Amino acid sequences with certain physico-chemical characteristics in terms of secondary structure propensities, hydrophobicity, charge trigger aggregation and amyloidosis.<sup>9</sup> Because their hydrophobic side chains are either randomly strewn or entirely buried out of touch with water, fully folded or unfolded proteins cannot combine effectively. The folding/unfolding intermediate's patches of adjacent hydrophobic groups are what first cause the aggregates to form. Protein molecules can group together just physically, without altering their fundamental structure or creating additional covalent bonds.<sup>7</sup> Proteins can aggregate when such a bond is formed, or it can indirectly change the original protein's propensity for aggregation. The amount of appropriately folded proteins produced during refolding can be dramatically decreased by protein aggregation. Even for aggregates of a single protein, protein molecules can take on a variety of forms and sizes. Protein aggregates are usually amorphous in nature. It has been discovered that numerous factors influence how proteins aggregate during refolding. These

include the following: temperature, protein concentration, denaturant type and concentration, and pH.<sup>6</sup> One of the better studied and significant factors that affects the beginning of aggregation and final aggregate morphology is pH. This is due to the fact that pH affects the surface charge of the protein monomer and the degree of any structural disruption prior to aggregation, which in turn affects their tendency to self-assemble and the way in which they aggregate. For instance, repulsive interactions between native monomers are diminished at pH levels near the isoelectric point, favouring assembly. In these circumstances, particles frequently develop. Increased charge repulsion inside the protein causes the folded conformation to become unstable at pHs outside of the isoelectric point, exposing hydrophobic groups that can then promote the self-assembly of these unfolded forms, generally forming  $\beta$ -sheet-rich fibrillar structures. Temperature is another important component, if not the most important one, in industrial procedures that cause aggregation. Raising the temperature causes proteins to vibrate more and diffuse more, two steps required for aggregation. In addition, the protein partially unfolds as the temperature approaches the denaturation temperature, exposing the hydrophobic areas that cause aggregation.<sup>8</sup> In many globular proteins, aggregation happens as a result of destabilizing circumstances or mutations, large concentrations, or situations in which denatured or partially folded forms are significantly populated.<sup>9</sup>

Proteins that are in their original state or that have partially or completely unfolded can start the creation of amyloid. Genetic changes that effectively destabilize the native state are frequently associated with the production of amyloid, indicating that a conformational change is the first crucial stage in amyloidogenesis.<sup>10</sup> Amyloid fibrils are insoluble proteinaceous substances that are present in a variety of protein-misfolding illnesses, such as prion disorders, Alzheimer's disease, and several types of systemic amyloidoses.<sup>12</sup> The long, mostly unbranched ribbon-like structure of amyloid fibrils is similar to that of morphology. Amyloids have a similar "cross- $\beta$ " architecture made up of laminated  $\beta$ - sheets at the molecular level. Because many polypeptides naturally possess the capacity to self-assemble into  $\beta$ -rich fibril structures, the prevalence of pathogenic amyloids is greatly increased. Interestingly, "functional amyloids" that are important components of bacterial, fungal, and mammalian cells also have cross- $\beta$  architecture. Amyloid fibrils also develop in endogenous proteins, where they carry out their typical duties. As proven from the simplest to most complex species, amyloid production is therefore not necessarily hazardous.<sup>11</sup> Both highly ordered fibrils and amorphous aggregates, which are both formed when proteins polymerize

and are linked to disorders characterized by protein misfolding, can develop when proteins are polymerized. The former is more common. Amorphous aggregates have a significant fraction of  $\beta$ -sheet structures. However, not all amorphous aggregates exhibit this pattern, which suggests that the production of amorphous aggregates requires an amyloid-like assembly mechanism that somehow fails to organize into higher order assemblies. The same protein can also polymerize into either linear amyloid fibrils or amorphous aggregates, depending on occasionally minor variations in the environmental factors, such as ionic strength and temperature, etc.<sup>5</sup>

Proteases are a significant class because they are widely used in the pharmaceutical, detergent, and food industries. They break down amide bonds, turning long-chain proteins into peptides and then amino acids. This method is widely used for cheese softening, beer clarity, and meat tenderization.<sup>13</sup> The drawback of using proteolytic enzymes in many applications is their temperature stability, which applies to both high and low temperatures.<sup>15</sup> Many physicochemical as well as structural phenomena find the study of surfactant-protein interaction to be quite interesting. Today, the soap and detergent industries make substantial use of proteolytic enzymes (enzymes that break peptide bonds). In the majority of protein-surfactant interactions, the "surfactant binding" to a single protein—which might unfold and occasionally denature the globular protein—is taken into account. Protein mixes containing anionic surfactants below and above the isoelectric point (IEP) and denatured proteins are two common examples that may occur. When the protein is below the IEP, it is referred to as a cationic biopolymer, and precipitation mechanisms dominate its interactions with anionic surfactants. Over the IEP, interactions have the potential to create completely soluble, stable complexes that can alter the protein's structure and conformation. Figure 1.3 shows the formation of amyloids above and below the isoelectric point of protein. More than cationic surfactants, SDS, the most popular anionic surfactant, causes proteins to unfold and denature.<sup>10</sup> The papain enzyme, a well-known member of the proteases group, is extensively used in the aforementioned applications. Papain speeds up wound healing, removes harmful microbes from the wound more quickly, and improves the environment for reparative processes. Papain is frequently employed in biological and biomedical research to examine the cell's receptor system, protein structure, chemical analysis, other physiologically active material purification methods.<sup>14</sup> Its key advantage over other proteases is that it has strong hydrolytic activity against a variety of protein substrates and that a sizable amount of it may be made from papaya fruit.<sup>18</sup> Papain demonstrated significant antioxidant action in addition to

being a protease, making its use in chemical manufacturing processes in the food sector particularly useful. These proteins' proteolytic activity has been utilized or inhibited for a variety of activities, including the processing of food and industrial materials, organic synthesis, cosmetic, and medicinal applications.<sup>15</sup> These enzymes are prospective targets for the development of tailored inhibitors because they have long been connected to numerous human illnesses. In comparison to other proteases, papain is less costly, has a broad range of specificity, and strong thermal stability.<sup>17</sup> It has a lot of potential to be used in detergents. Papain molecules weigh ~23.4 kDa and have an isoelectric point of 9.02 with three disulfide bridges and catalytically important cysteine (position 25), Asparagine (position 175) and histidine residues (position 158). The 212 amino acid residues that make up papain molecules are folded into two halves to produce a cleft.<sup>16</sup> The study of intermediate species and the unfolding/refolding process of mature cysteine proteases, used in various biotechnological applications, has recently attracted fresh interest. Understanding how proteins interact with surfactants is crucial because it gives us insight into the way papain and SDS bind to one another and how it affects the structure and function of proteins. The goal of this study was to develop a straightforward legislative method to use SDS to induce protein aggregation or amyloid formation under the right conditions. The resulting aggregates were examined using a variety of spectroscopic and microscopic techniques, including circular dichroism, intrinsic fluorescence, Thioflavin T (ThT) binding, ANS fluorescence, scanning electron microscopy, and transmission electronic microscopy.

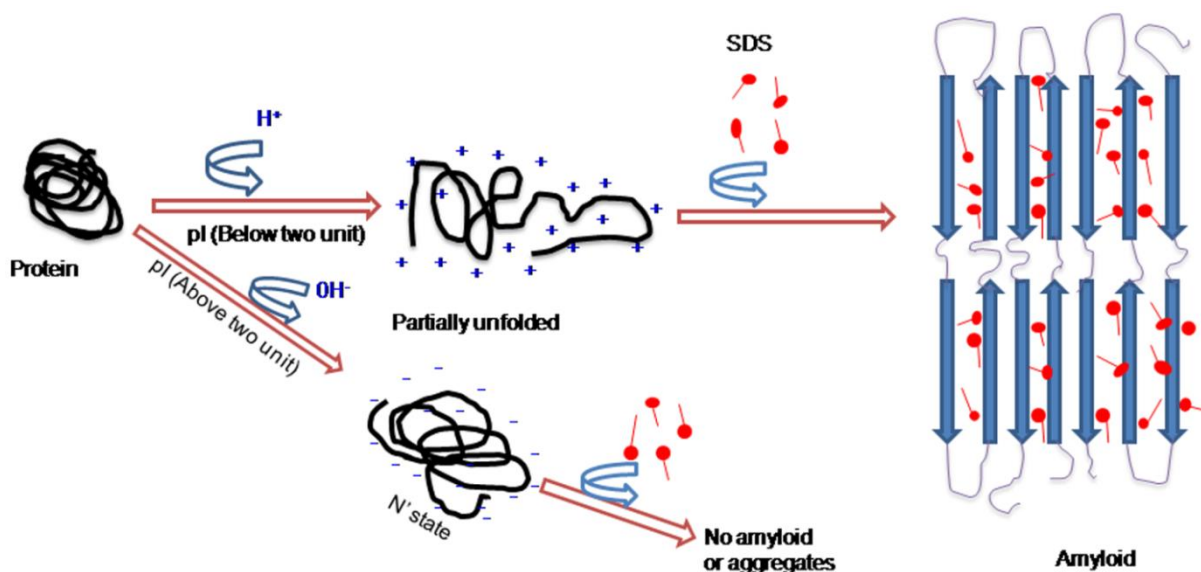


**Figure 1.3:** Formation of amyloids, above and below the pI. Adaped from Khan J.M.; Khan R.H. SDS can be utilized as an Amyloid Inducer: A case study on diverse proteins. PLoS ONE 2012, 7.

## LITERATURE REVIEW

The active principle in papaya latex was initially studied by Wurtz and Bouchut in 1879 in a carefully controlled scientific study. These writers utilised fresh latex and identified two distinct components: the liquid latex and the pulp. The process yielded a white amorphous powder that became known as "papain" and was considered the purest form of the active component.<sup>23</sup> Several plants of proteinase family have been reported in the past to generate partially denatured structural states at low pH, including the molten globule and A-states.<sup>19</sup> Due to its molecular structure and several industrial applications, papain, a sulfhydryl protease extracted from *Carica papaya* latex, has been the subject of much research. Papain is a cysteine proteinase that consists of a single polypeptide chain with 212 amino acid residues folded into a globular protein with two distinct domains: L, with residues 10-111 and 208-212, and R, with residues 1-9 and 112-207. Figure 2.1 shows the primary sequence of papain contains different amino acid residues. Methionine is absent in papain.<sup>20</sup>

<b>1</b>	<b>11</b>	<b>21</b>	<b>31</b>	<b>41</b>
<b>IPEYVDWRQK</b>	<b>GAVTPVKNQG</b>	<b>SCGSCWAFSA</b>	<b>VVTIEGIIKI</b>	<b>RTGNLNQYSE</b>
<b>51</b>	<b>61</b>	<b>71</b>	<b>81</b>	<b>91</b>
<b>QELLDCDRRS</b>	<b>YGCNGGYPWS</b>	<b>ALQLVAQYGI</b>	<b>HYRNTYPYEG</b>	<b>VQRYCRSREK</b>
<b>101</b>	<b>111</b>	<b>121</b>	<b>131</b>	<b>141</b>
<b>GPYAAKTDGV</b>	<b>RQVQPNQGA</b>	<b>LLYSIANQPV</b>	<b>SVVLQAAGKD</b>	<b>FQLYRGGIFV</b>
<b>151</b>	<b>161</b>	<b>171</b>	<b>181</b>	<b>191</b>
<b>GPCGNKVDHA</b>	<b>VAAVGYGPNY</b>	<b>ILIKNSWGTG</b>	<b>WGENGYIRIK</b>	<b>RGTGNSYGVC</b>
<b>201</b>	<b>211</b>			
<b>GLYTSSFYPV</b>	<b>KN</b>			

**Figure 2.1:** Representation of primary sequence of papain.

<b>Amino acids</b>	<b>No. of residues</b>	<b>Amino acids</b>	<b>No.of residues</b>
<b>Pro (P)</b>	10	<b>Asn (N)</b>	13
<b>Gln (Q)</b>	13	<b>Leu (L)</b>	11
<b>Thr (T)</b>	8	<b>Arg (R)</b>	12
<b>Ala (A)</b>	14	<b>Phe (F)</b>	4
<b>Ser (S)</b>	13	<b>His (H)</b>	2
<b>Glu (E)</b>	7	<b>Cys (C)</b>	7
<b>Ile (I)</b>	12	<b>Met (M)</b>	0
<b>Val (V)</b>	18	<b>Gly (G)</b>	28
<b>Lys (K)</b>	10	<b>Trp (W)</b>	5
<b>Tyr (Y)</b>	19	<b>Asp (D)</b>	6

**Figure 2.2:** Number of amino acid residues in papain.

The substrates attach in a deep gap between the two domains, close to the active-site cysteine (Cys-25) and histidine (His-159) residues.<sup>21</sup> Hydrophobic cores, to which numerous side chains contribute, are likely responsible for some of the structural stability of each lobe. Some evidence suggests that papain is composed of two lobes, with the folding of one lobe occurring independently of the other. The polypeptide chain appears to fold in two distinct ways between the lobes.<sup>22</sup> In the L domain,  $\alpha$ -helices predominate. Anti-parallel  $\beta$ -sheet structure is the defining characteristic of the R domain.<sup>20</sup>

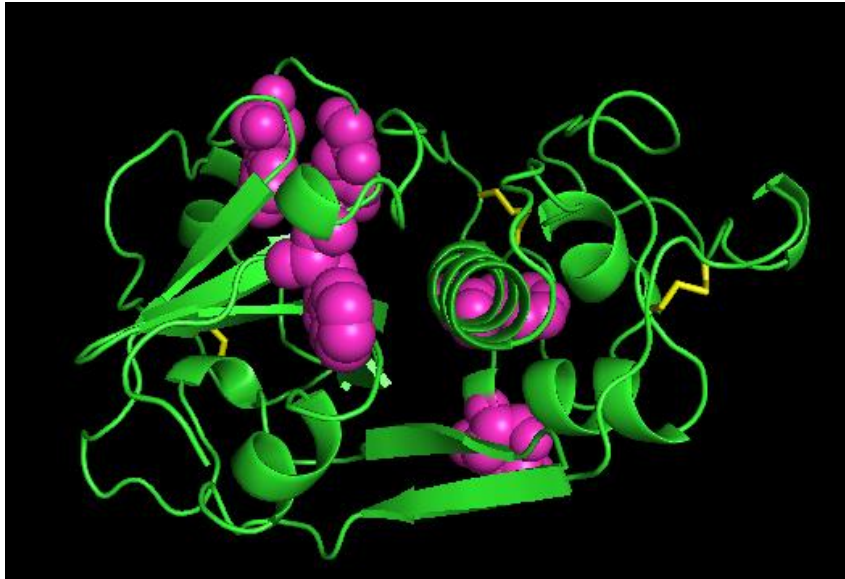


**Figure 2.3:** Ribbon diagram of papain (PDB: 1BQI) Pink colour shows the tryptophan amino acid residue present in papain and yellow colour shows the disulfide bonds in papain.

Compact globularity of the molecule with native-like secondary structure but unfolded tertiary structure characterises the intermediate term as "molten globule" describes this state.<sup>24</sup> The enzyme exhibits a distinct preference for hydrolyzing peptide bonds that involve amino acid residues with basic side chains, mostly arginine and lysine, as well as those that follow phenylalanine. To determine the relative hydrophobicity and hydrophilicity values in protein sequence is quite useful. The distribution of hydrophobic and hydrophilic residues within a protein can provide insights into its tertiary structure, as hydrophobic residues are typically buried in protein core while hydrophilic residues are more likely to be found on the protein surface. Protein conformation is primarily influenced by hydrophobic interactions. The amino acid side chains that exhibit the highest hydrophobicity include alanine, valine, leucine, methionine, and isoleucine, which display varying degrees of hydrophobic character. The dominant thermodynamic forces that facilitate protein folding are attributed to the hydrophobic-hydrophilic interaction of papain amino acids in the side chain.<sup>25</sup> The experiment shows that SDS, at varying concentrations, exerts a significant influence on the formation of two distinct intermediates through distinct thermodynamic pathways through hydrophobic interactions (Chamani et al., 2009). However, it exhibits a preference for amino acids that possess a large hydrophobic side chain at the P2 position, while it does not accommodate Val in P1 (Kamphuis et al., 1985).<sup>27</sup> The enzyme exhibits enhanced stability in

hydrophobic solvents and reduced water content, and retains its substrate specificity while catalysing reactions in diverse organic solvents (Stevenson and Storer, 1991).<sup>28</sup>

CD spectroscopy and fluorescence experiments demonstrate that at pH 2, papain changes from its native state into a molten globule state.<sup>22</sup> Based on the discovery that acid unfolded papain regains, upon neutralisation, the spectral features of the native state, refolding of papain from the A and molten globule states to the native state has been described as entirely reversible.<sup>22</sup> Most acid denaturation processes that have been studied so far have also been demonstrated to be reversible.<sup>30</sup> Papain's thermal unfolding at pH 2–2.6 was quite reversible, in stark contrast to pH 7, when aggregation was clearly observable.<sup>22,31</sup> Papain in the molten globule state undergoes a non-cooperative thermal unfolding with biphasic transition curves. The A-State transitions to the molten globule state at pH 2, and back to the native state as the pH rises to the 4-10 range.



The reversible conversion of the native state of papain into partially structured states at acidic pH.

Later, it was observed that the addition of urea at pH 2 caused papain acid denaturation to be irreversible.<sup>30</sup> When the pH is low, even in the presence of a little amount of salt or denaturant, molten globules have a strong tendency to stay together and form larger aggregates. Similarly, in the presence of 0.5 M to 1.2 M GuHCl, papain aggregated from its molten globule state, with the amount of the aggregation decreasing with increasing denaturant concentration.

Recent research has showed that the natural shape of a protein undergoes partial unfolding as the initial stage in the aggregation process. The formation of aggregates is facilitated by the increased exposure of certain areas, such as hydrophobic sites or free SH groups, to novel intermolecular interactions. Concentration-dependent effects of ionic surfactants, especially sodium dodecyl sulphate (SDS), on the aggregation behaviour of proteins was well-documented. It was discovered that SDS did not restore the protein's function by suppressing aggregation. Incubation of papain with a postmicellar SDS concentration renders the enzyme inactive. At a neutral pH of 7.0, the enzyme papain underwent thermal unfolding in the absence of the surfactant SDS and at temperatures ranging from 50 °C to 80 °C, resulting in the formation of disordered protein aggregates. Above 50 °C, the presence of 6 mM SDS

reduced enzyme activity by nearly a factor of 10. These results suggest that SDS might have prevented damage to the protein secondary structure but severely disrupted its tertiary conformation, which is essential for the enzyme activity. In light of the foregoing, it can be concluded that the conformational modifications brought about by SDS, making papain structurally stable but rendering it functionally inactive. Fig. 2.4 is a schematic representation of the study's overall findings.<sup>32</sup>

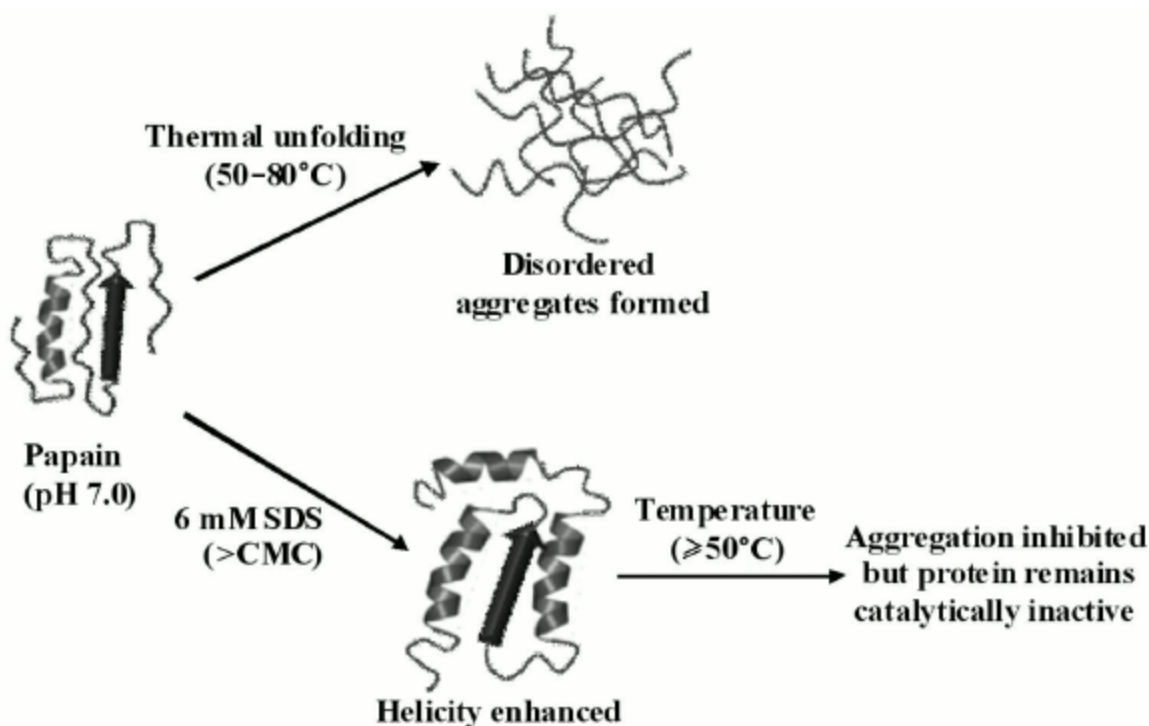


**Figure 2.4:** Schematic representation of temperature-induced changes in papain conformation in the absence and presence of SDS. Adapted from Qadeer A.; Khan R.H. The inhibitory effect of Post- Micellar SDS concentration on Thermal Aggregation and Activity of Papain. *Biochemistry (Moscow)* **2014**, 79, 785- 796.

At pH 2, papain in molten globule conformation exhibits a propensity for aggregation in the presence of low concentrations of  $\text{GnHCl}$ . However, the addition of SDS at low concentrations effectively prevents this aggregation and promotes protein stabilisation. The hydrophobic chain length of SDS correlates with the stabilisation and prevention of aggregation in the molten globule state of papain.<sup>34</sup> Multiple modes of association have been observed in surfactant-protein interactions, which can be attributed to dipole-dipole, ion-dipole, or ion-ion forces. Six different types of associations are discussed by Nagarajan et al.. The endothermic nature of the interaction between SDS and papain was observed and confirmed through calorimetry.<sup>34</sup> The interaction of SDS with papain is an entropy-

controlled process. The proteolytic enzyme papain exhibits remarkable thermal stability and resistance to denaturing agents, including 8 M urea and 70% EtOH.<sup>35</sup> The conformation of acid-unfolded papain varies in the presence of various detergents, thereby providing distinct information that can be utilised for protein purification purposes. The fundamental function of detergents in the process of protein purification is to induce solubilization. Under acidic conditions and in the presence of SDS, ANS binding was observed to be reduced in comparison to the acid-unfolded papain or the Tween-induced state. In the near-UV region of the CD spectrum, indicating a possible ordering of the tertiary structure. In the case of Tween, an intermediate conformation exhibiting secondary structure, accompanied by loss of tertiary structure and increase in ANS binding affinity, was observed. The present state under consideration exhibits characteristics similar to molten-globule state. Regarding CTAB, the resultant intermediate state may be identified as a molten globule, as a consequence of increase in ANS binding and a secondary structure that maintains native-like tertiary contacts. The impact of surfactants on polypeptides depends upon the characteristics of both the surfactant and the protein moiety. Furthermore, the environmental factors play a crucial role. The experimental data suggests that SDS and CTAB are superior detergents, as evidenced by protein regains of both secondary and tertiary protein structures.<sup>36</sup>

## CHAPTER 3

### MATERIALS AND METHODS

#### **3.1 Reagents used**

Powdered papain (latex papaya) was bought from Sigma-Aldrich (P4762). Thioflavin T (ThT) and ANS (8-anilinonaphthalene-1-sulphonic acid) were purchased from Sigma Aldrich. Materials for buffer formulations, such as monobasic phosphate and dibasic diphosphate, were also purchased from Sigma-Aldrich, along with sodium dodecyl sulphate (SDS). All reagents were of the highest purity and utilised exactly as they were obtained.

#### **3.2 Glassware and labware used**

Micropipettes (Eppendorf Research), micropipette tips, microcentrifuge tubes (MCTs), for recording fluorescence spectra 10×10 mm with stopper whereas for recording Circular Dichroism (CD) spectra, 10×1 mm cuvettes were used, reagent bottles, kim wipes, , falcon tubes, gloves.

#### **3.3 Methodologies:**

##### **3.3.1 Analysis of Sequence Statistics**

Papain aggregation properties were anticipated using its amino acid sequence and bioinformatics software. Scripps Calculator (<http://protcalc.sourceforge.net/>), was used to estimate charge over the pH range and isoelectric point. PONDr (<http://www.pondr.com/>) were used to forecast the disordered regions and the level of disorder in papain. The Net Charge per Residue in a protein was visualised with CIDER (<http://pappulab.wustl.edu/CIDER/analysis/>), a programme designed to depict protein polarity. Aggrescan ( [Aggrescan: Prediction of "hot spots" of aggregation in polypeptides \(uab.es\)](http://uab.es) ) was used to examine the aggregation tendency of papain, with the resulting maps illustrating the locations of the hottest regions.

##### **3.3.2 Stock Solutions Preparation**

**Dibasic diphosphate Buffer preparation:** Stock solutions were made with milli-Q water, the purest water available, and reagents were of analytical quality. Dibasic diphosphate buffer (mol wt. 177.99 g/mol) was diluted in milli-Q water to create a 500 mM buffer stock. In addition, 20 mM concentration sub-stocks of dibasic diphosphate buffer at pH 7.4 were

generated by diluting the concentrated stock with milli-Q water. Buffers had their pH altered with hydrochloric acid. The final pH of all the buffers were maintained within the error of  $\pm 0.02$  at room temperature using a Cyberscan510 pHmeter (Eutech Pvt. Ltd.) and was stored in the fridge at 4 °C.

**Monobasic phosphate Buffer preparation:** Stock solutions were made with milli-Q water, the purest water available, and reagents were of analytical quality. Monobasic phosphate buffer (mol wt. 156.01 g/mol) was diluted with milli-Q water to create a 500 mM buffer stock. In addition, 5 mM concentration sub-stocks of monobasic phosphate buffer at pH 7.0 were generated by diluting the concentrated stock with milli-Q water. Buffers had their pH altered with NaOH. The final pH of all the buffers were maintained within the error of  $\pm 0.02$  at room temperature using a Cyberscan510 pH meter (Eutech Pvt. Ltd.). All buffers were stored in the fridge at 4 °C.

**Papain Stock solution preparation:** Papain (weighted 23.4 kDa, per literature) is weighed out in a micro-centrifuge tube and diluted in monobasic phosphate buffer (pH 7.0, 5 mM) to make up the volume necessary to generate the protein stock solution. Protein concentration was determined using a Shimadzu UV-2600 spectrophotometer equipped with 500  $\mu$ L cuvettes. In order to calculate absorbance, the value of extinction coefficient =  $58,515 \text{ M}^{-1} \text{ cm}^{-1}$  at 280 nm was used.

**Sodium dodecyl sulfate stock solution preparation:** The SDS (10 mM) stock solution is made by weighing out the required amount of SDS into a micro-centrifuge tube, then diluting it with milli-Q water to reach the required volume. The SDS was stored at temperature 25 °C.

**Preparation of Extrinsic Fluorescent Dyes:** ThT and ANS dyes were both prepared in 10 mM stock solutions and kept at -20 °C for later use. In addition, 1 mM sub-stocks of ThT and ANS were made by diluting them in milli-Q water by 10-folds, and stored in the fridge at 4 °C. The reaction mixture used for the spectroscopic experiments had a working concentration of 10  $\mu$ M.

### **3.3.3 Steady-State Fluorescence measurements:**

To examine the environmental changes in the protein as a function of time, fluorescence studies were carried out using the Shimadzu RF-6000 Fluorescence Spectrophotometer at  $\sim 25$  °C. To monitor the aggregation kinetics, a well-known amyloid indicator namely,

Thioflavin-T (ThT) was used. ThT shows a strong fluorescence enhancement at 480 nm indicating the formation of fibrillar aggregates as a function of time. The reaction mixture was prepared in a cuvette (10×10 mm) at pH 7.4, 25 °C using dibasic diphosphate buffer (20 mM). The reaction volume used for our reactions was 2.5 mL. We first monitored the fluorescence with the ThT probe in both papain and SDS concentration dependence manner. First, using a constant papain protein concentration of 5 μM, we looked at SDS dependent concentration as a function of time. For these studies, reaction mixture of 2.5 mL was prepared in the cuvette. Dibasic buffer (20 mM) was added first, followed by ThT (10 μM), and then 5 μM of protein and reaction mixture was mixed well. An excitation wavelength of 450 nm and an emission wavelength of 480 nm were used to measure the ThT Fluorescent intensity. The spectra were recorded between 470 -560 nm. The data interval was set to 1, the slit width was 5.0 and 5.0 nm for both excitation and emission, and the scan speed was 600 nm/min. The spectra was recorded in absence and presence of SDS as a function of time. Different concentrations of SDS used were: 300 μM, 500 μM, 1 mM, and 2 mM. In the same manner, papain concentration dependent studies were performed, keeping the SDS concentration constant (1 mM). For the preparation of reaction mixture, Dibasic buffer (20 mM) was added first, followed by ThT (10 μM), and papain. Different concentrations of papain used for the studies were: 2 μM, 5 μM, 10 μM, 25 μM and 50 μM. The spectra was recorded in absence and in presence of 1mM SDS using the above mentioned ThT parameters. We also took advantage of one intrinsic fluorophore i.e. Tryptophan and the parameters used for recording tryptophan spectra were: excitation wavelength: 295 nm and emission wavelength: 335 nm. The emission range used for recording the spectra was: 320-450 nm. Further, to monitor the changes in protein hydrophobicity another extrinsic fluorophore namely, ANS was used. Studies were performed in both, protein and SDS concentration dependent manner, using same concentrations, as used for ThT studies. The procedure for preparing and analyzing the reaction mixture was also the same as for ThT. An excitation wavelength of 350 nm and an emission wavelength of 475 nm were used to measure the ANS fluorescence intensity. The spectra were recorded between 400-600 nm. The data interval was set to 1, the slit width was 5.0 nm for excitation and 5.0 nm for emission, and the scan speed was 600 nm/min.

To examine the rotational flexibility of tryptophan in the protein, we have carried out fluorescence anisotropy measurements as a function of time using Horiba Jobin Yvon

Fluoromax-4 Fluorescence Spectrophotometer at ~25 °C. The fluorescence anisotropy is expressed as follows:

$$r_{ss} = (I_{\parallel} - GI_{\perp}) / (I_{\parallel} + G2I_{\perp})$$

where  $I_{\parallel}$  and  $I_{\perp}$  denotes the emission polarizer oriented parallel and perpendicular and  $G$  denotes the geometrical factor which was used to correct the perpendicular components. Firstly, we monitored tryptophan anisotropy by keeping constant concentration of papain of 5  $\mu\text{M}$  and varying the concentration of SDS (0.2 – 2 mM) as a function of time. Further, we carried out tryptophan anisotropy measurements in a papain concentration-dependent manner (5 – 50  $\mu\text{M}$ ) in the presence of 1 mM SDS. The tryptophan fluorescence anisotropy parameters were: excitation wavelength: 295 nm and emission wavelength: 335 nm. The data interval was set to 1, the slit width was 3.0 nm for excitation and 3.5 nm for emission, and the scan speed was 60 nm/min. All these experiments were repeated at least three times.

**3.3.4 Circular Dichroism measurements:** To examine the secondary structural changes in the protein as a function of time, CD studies were carried out using the Chirascan CD Spectrophotometer (Applied Photophysics, UK) at 25 °C. The reaction mixture was prepared in an eppendorf at pH 7.4 and at RT using dibasic diphosphate buffer (20 mM). The experiments were performed in similar manner as ThT and ANS. First, the spectra was collected only for dibasic diphosphate buffer and then the protein (5  $\mu\text{M}$ ) was added and spectra was collected again. Finally, required amount of SDS was added and then the spectra were collected as a function of time. The reactions were performed at different concentrations of SDS: 200  $\mu\text{M}$ , 300  $\mu\text{M}$ , 500  $\mu\text{M}$ , 1 mM, and 2 mM. All the far- UV CD spectra were recorded in the range of 195- 260 nm. 1.0 nm/s scan speed with a 1 nm bandwidth. The final spectrum, which represented the average of five scans, was corrected by subtracting the contribution of buffer in the specified wavelength range, smoothed using the Savitzky-Golay method in the ProData software provided with the CD spectrophotometer, and then replotted in OriginPro.

### **3.3.5 Zeta Potential measurements:**

The zeta potential measurements were carried out on a Malvern Zetasizer Nano ZS (Malvern, UK) at ~25 °C. The reaction volume used for our studies was 1 mL. The measurements were collected in SDS concentration dependent manner, keeping the protein concentration constant at 5  $\mu\text{M}$ . The Smoluchowski method was used to determine the zeta potential of sample

mixture. Every measurement was the average of three scans, and every experiment was run independently at least three times.

### **3.3.6 Field Emission Scanning Electron Microscopy (FESEM):**

FESEM images were analysed to determine the morphology of papain aggregates. Field emission scanning electron microscopy (FESEM) was performed on Sigma 500 Gemini 1 (Zeiss). The images were collected at 5  $\mu\text{M}$  and 50  $\mu\text{M}$  of papain, keeping the SDS concentration constant at 1 mM. The images were also collected at 300  $\mu\text{M}$  and 1 mM SDS, keeping the papain concentration constant at 5  $\mu\text{M}$ . The reactions were incubated for 3 hours at RT. The reaction mixtures were centrifuged at 8000 rpm for 15 minutes at 25 °C. The supernatant was removed and the resulting pellet was resuspended in 100  $\mu\text{L}$  of pH 7.4 dibasic phosphate buffer, which was further diluted by 50 folds in Milli-Q water. 5  $\mu\text{L}$  of the diluted sample was dropcasted on the coverslip and dried for overnight at RT. The samples were coated with gold using a Quorum 150R ES Plus before carrying out SEM imaging. The SEM images were taken using the SmartSEM software that was included with the equipment, and imaging was carried out using an acceleration voltage of 5 kV with a magnification range of 500 nm- 1  $\mu\text{m}$ .

### **3.3.7 Transmission Electron Microscopy (TEM):**

Along with FESEM, TEM images were also collected for determining the morphology of the aggregates. The samples were prepared for 5 and 50  $\mu\text{M}$  concentrations of papain keeping the SDS concentration constant to 1 mM and incubated at RT for 2.5 hours. Then, these reaction mixtures were centrifuged for 20 minutes at room temperature at 16400 revolutions per minute at RT. The resulting pellet was redissolved in milli-Q water and the supernatant was discarded. After being adsorbed on a 300-mesh carbon-coated electron microscopy grid for 2.5  $\mu\text{L}$  of the resuspended solution, the grid was stained with 2.5  $\mu\text{L}$  of uranyl acetate (1%), incubated for 5 min, and then excess stain was removed with a kimwipe. The grid was then allowed to dry overnight at room temperature, and the morphology was examined under a microscope with 40,000 magnification at 200 KV acceleration voltage on Jeol JEM-F200 at room temperature.

## CHAPTER 4

### RESULTS AND DISCUSSIONS

We used different bioinformatic tools to analyse papain intrinsic nature and get knowledge on its sequence properties and aggregation properties.

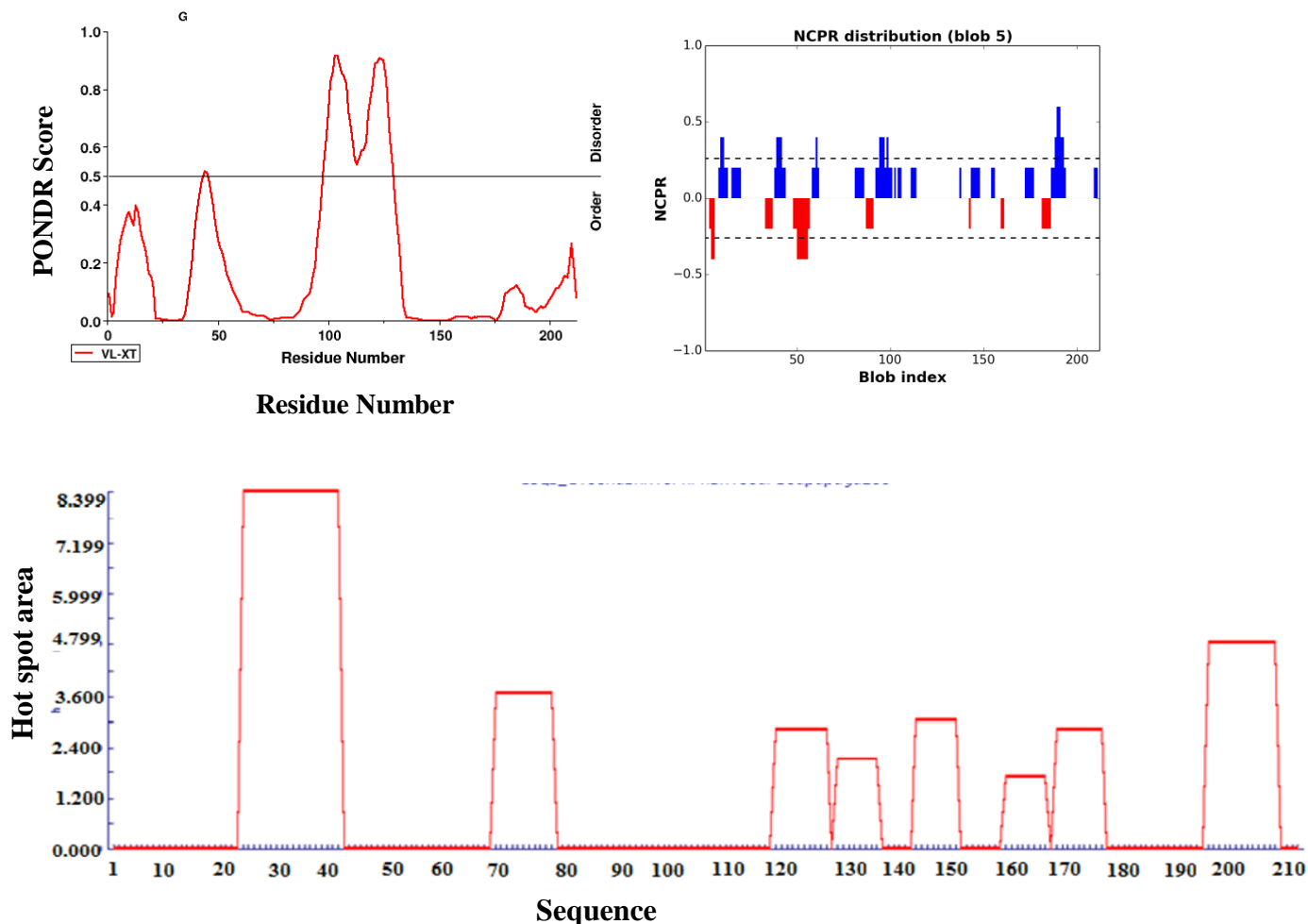


**Figure 4.1:** Bioinformatic tools representing the disorderedness using (a) PONDR; (b) charge distribution w.r.t Blob index using NCPR; (c) AGGRESCAN analysis representing hotspot areas.

The PONDR plot gives information about the natural disordered regions in a protein. Fig. 4.1(a) shows the disordered and ordered regions of papain based on the PONDR Score. The regions above threshold shows disordered while below threshold shows the ordered regions. Fig 4.1(b) NCPR shows the fraction of positively and negatively charged residues. From this, we can say that papain protein has more positively charged residues. Fig 4.1 (c)

AGGRESCAN plot gives us the information about the amino acid residues which has higher propensity to aggregate, known as “hot spot regions”. The sequence analysis suggests that papain shows higher propensity to undergo aggregation. The data also reveals that these hot spot areas are basically dominated by non polar amino acid residues which indicates that the aggregation is predominantly driven by hydrophobic interactions. To elucidate the role of the interactions during aggregation, we have used a host of spectroscopic and microscopic tools in order to investigate the formation of aggregates upon addition of varied concentration of SDS at pH 7.4.

### SDS-induced aggregation of Papain: SDS concentration dependence

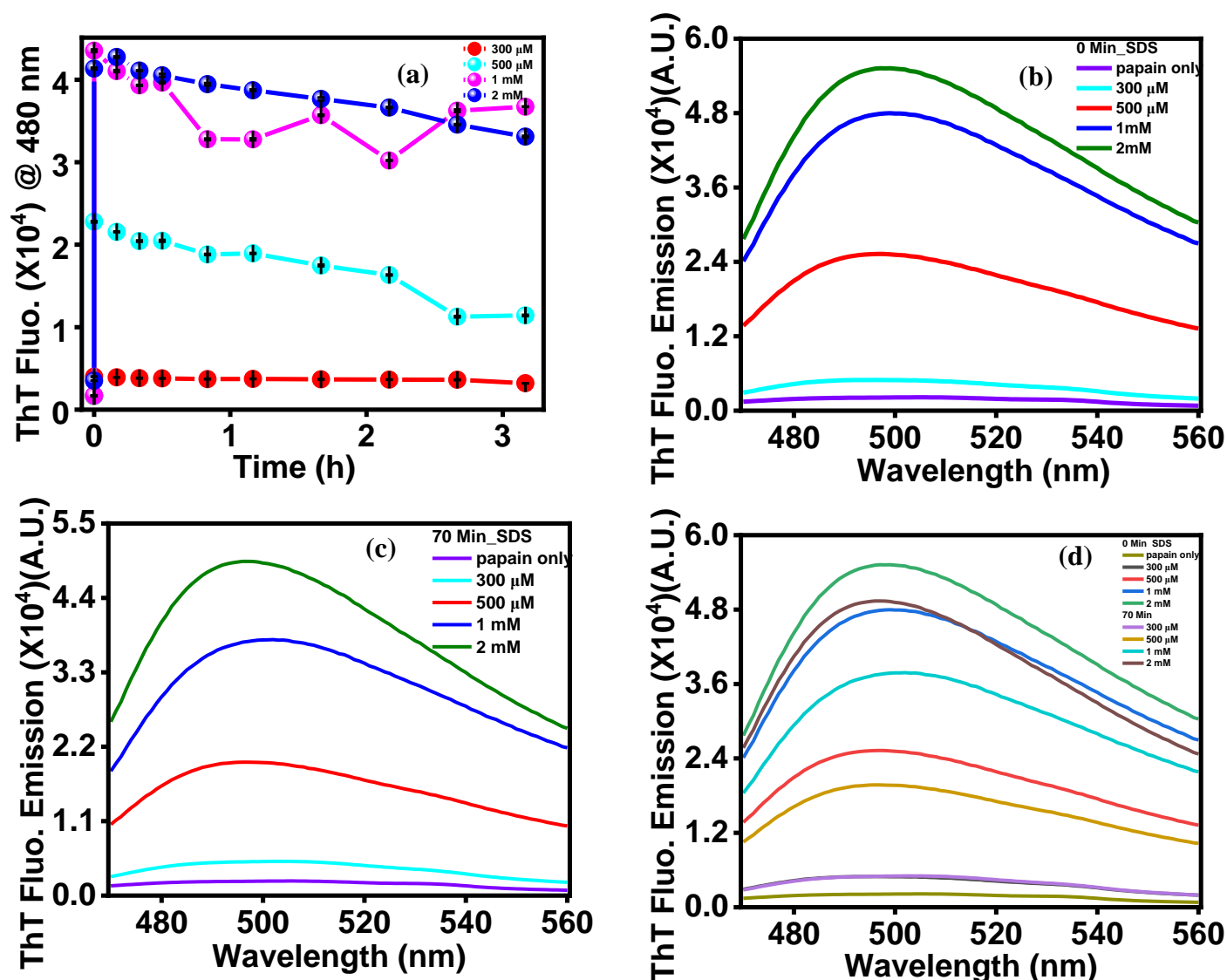


**Figure 4.2** (a) ThT fluorescence kinetics monitored at 480 nm at 5  $\mu$ M papain, in absence and presence of variable SDS concentration. (b) and (c) shows the ThT fluorescence spectra at 0 min and 70 min in the absence and presence of variable SDS concentration. (d) shows the combined plot of ThT fluorescence spectra at 0 min and 70 min.

In order to check whether the amyloids were formed or not, we used ThT fluorescence probe, which is a well-known amyloid marker and shows the emission maxima at 480 nm. In the absence of SDS, there was no significant change but upon addition of SDS there was an abrupt increase in ThT fluorescence intensity, which reached an apparent saturation; fig 4.2 (a). The extent of increment in fluorescence intensity was directly dependent on SDS concentration. We have also collected the spectra and noticed that the ThT fluorescence maxima was not at 480 nm, instead it was red-shifted to ~497 nm; fig. 4.2 (b), (c), (d). Based on these experiments, we observed that SDS was indeed inducing papain aggregation but they were not amyloids, because these aggregate did not exhibit cross- $\beta$  characteristic.

### **SDS-induced aggregation of Papain: Protein concentration dependence**

Similarly, we performed papain concentration dependent experiments by keeping the SDS concentration constant at 1 mM, in order to determine how the protein concentration was affecting the aggregation phenomenon. We observed that only papain in absence of SDS also showed slight increase in fluorescence intensity but in the presence of 1 mM SDS there was a phenomenal increase in ThT fluorescence intensity which showed directly proportional to the protein concentration; fig. 4.3(a), (b), (c), (d). We also observed that the ThT fluorescence maxima was not at 480 nm as observed earlier. Based on ThT fluorescence studies we suggest that there was an enhancement in aggregation process upon increment in concentration of either the protein or SDS.

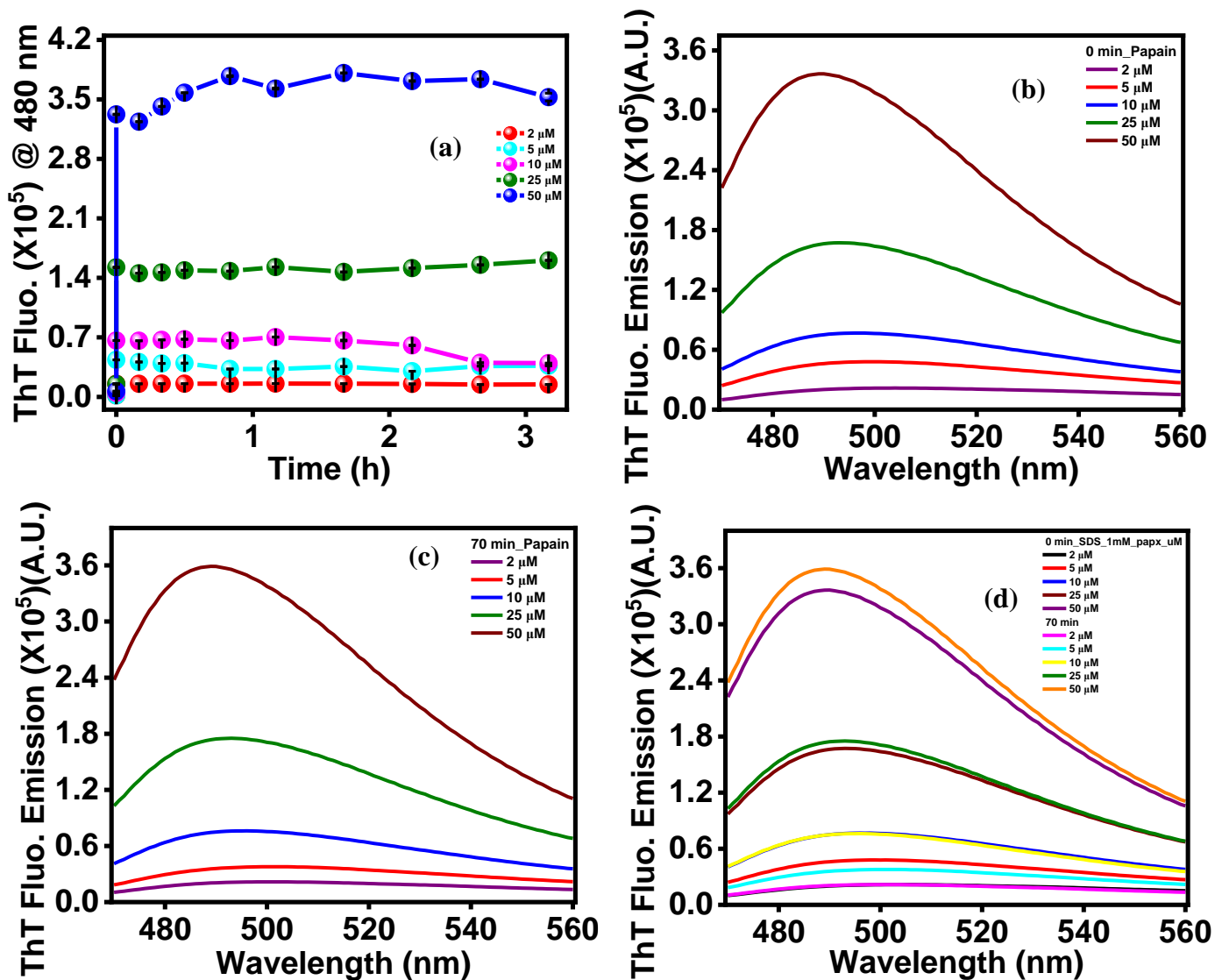


**Figure 4.3** (a) ThT fluorescence kinetics monitored at 480 nm in absence and presence of 1 mM SDS, for variable papain concentration. (b) and (c) shows the ThT fluorescence spectra at 0 min and 70 min in presence of 1 mM SDS and variable protein concentration. (d) shows the combined plot at 0 min and 70 min.

### SDS-induced environment changes of Papain: SDS concentration dependence

In order to investigate the local environment polarity and conformational changes in protein, the steady state fluorescence emission of five tryptophan residues was recorded. In the absence of SDS, there was no change in tryptophan fluorescence intensity but in the presence of SDS there was decrease in tryptophan fluorescence intensity; fig 4.4 (a). We have also collected the spectra which shows that there was decrease in the tryptophan fluorescence emission which suggested that there was some changes in the vicinity of tryptophan. At the same time the fluorescence emission was not exactly at 335 nm instead there was a blue shift of around 5-7 nm, which suggests that tryptophan(s) are experiencing the hydrophobic environment;fig. 4.4 (b), (c), (d).

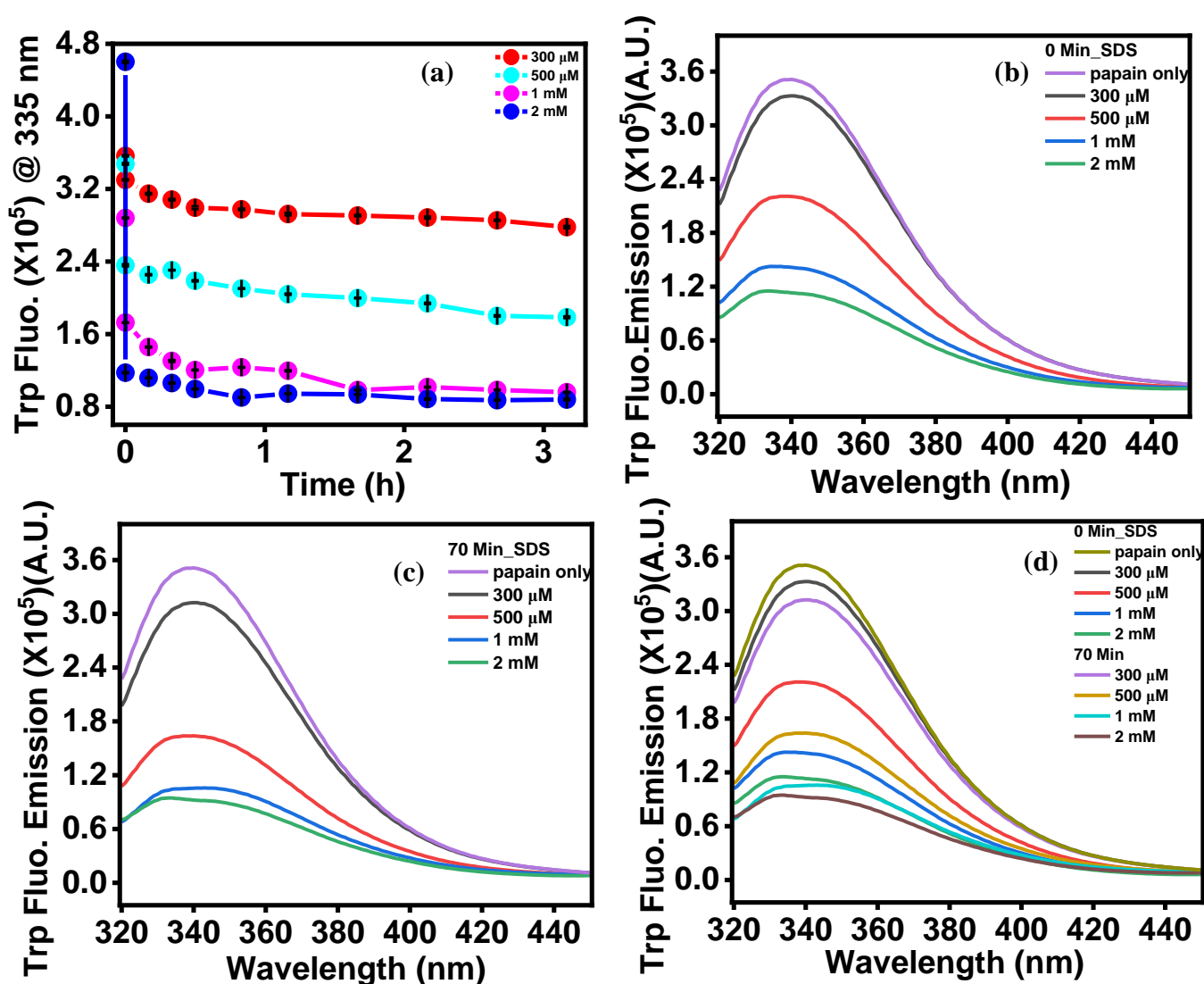


**Figure 4.4** (a) Tryptophan fluorescence kinetics monitored at 335 nm, at 5 μM papain, in absence and presence of variable SDS concentration. (b) and (c) shows the tryptophan fluorescence spectra at 0 min and 70 min in the absence and presence of variable SDS concentration. (d) shows the combined plot at 0 min and 70 min.

### SDS-induced environment changes of Papain: Papain concentration dependence

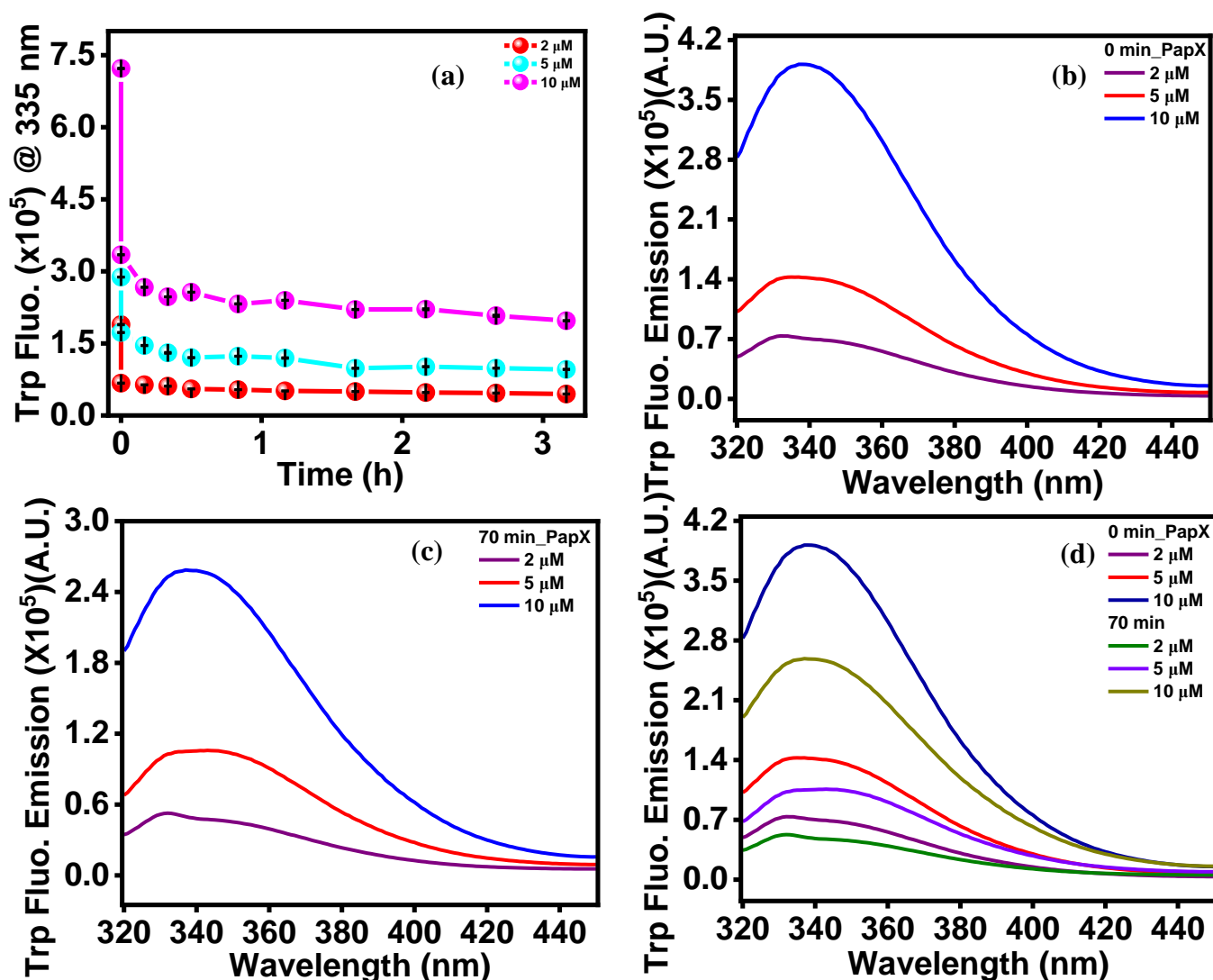


**Figure 4.5** (a) Tryptophan fluorescence intensity at 335 nm as a function of time in absence and presence of 1 mM SDS, at varied papain concentration. (b) and (c) shows the tryptophan fluorescence emission at 0 min and 70 min presence of 1 mM SDS and varied protein concentration. (d) shows the combined plot at 0 min and 70 min.

To examine how the protein concentration was impacting the local environment around tryptophan residues, we also conducted papain concentration dependent experiments while SDS concentration was kept constant at 1 mM. Tryptophan fluorescence intensity increased with an increase in papain concentration in the absence of SDS, but it decreases in the presence of SDS; Fig. 4.5(a). The spectra shows that tryptophan fluorescence emission increased as papain concentration increased, but that the emission was not precisely at 335 nm but rather had a red shift of 6-8 nm; fig. 4.5 (b), (c), and (d). We conclude that some

tryptophan may get buried in the hydrophobic environment and some tryptophan may get exposed to the hydrophilic environment.

**SDS-induced hydrophobic changes of Papain: SDS concentration dependence**

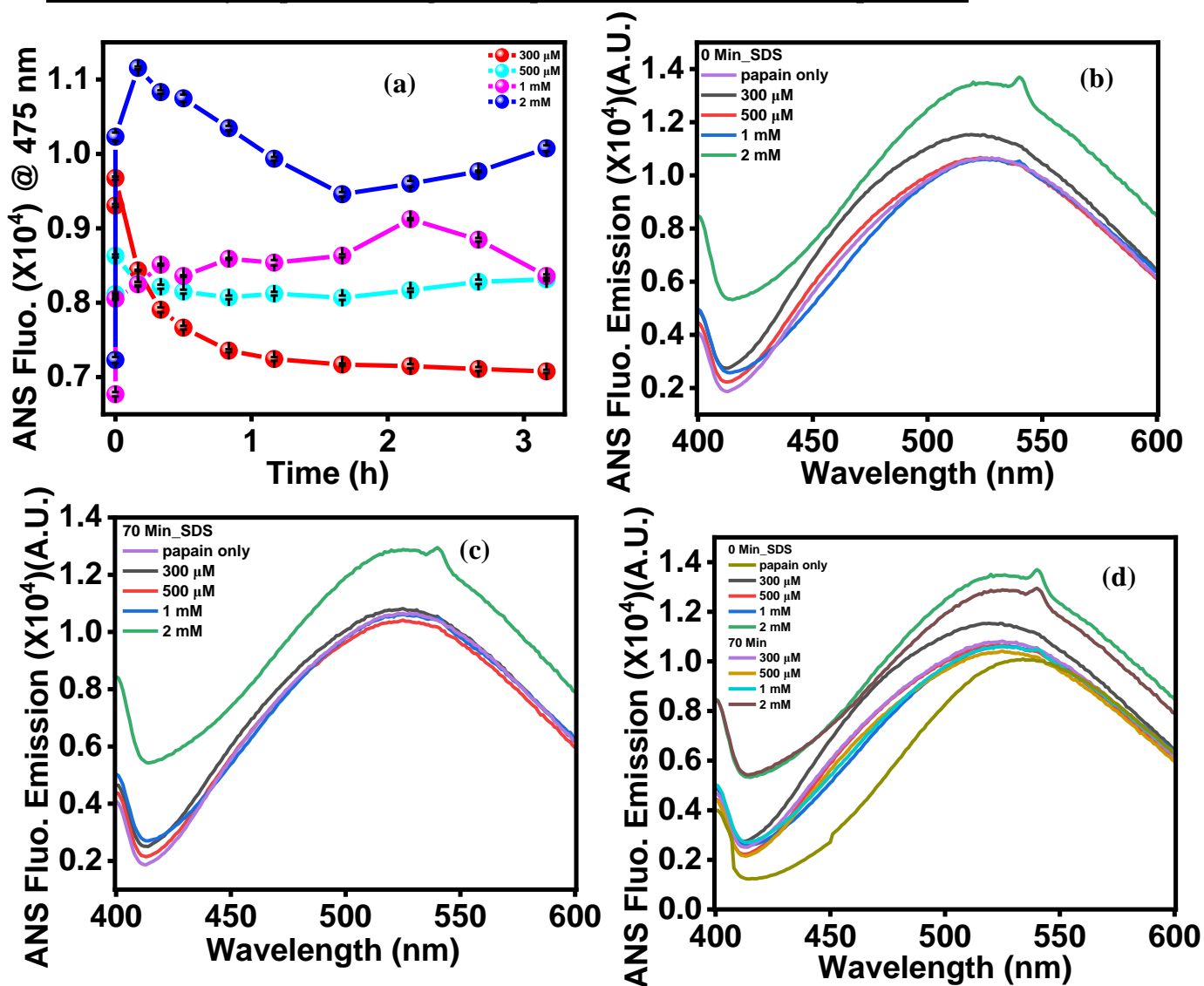


**Figure 4.6** (a) ANS fluorescence kinetics monitored at 475 nm at 5 μM papain, in absence and presence of variable SDS concentration. (b) and (c) shows the ANS fluorescence spectra at 0 min and 70 min in the absence and presence of variable SDS concentration. (d) shows the combined plot of ANS fluorescence spectra at 0 min and 70 min.

ANS was used as an extrinsic fluorophore to further analyse the aggregation of papain. We did not observe any change in the absence of SDS but in the presence of SDS, we observe a slight change at higher concentration; fig. 4.6 (a). Additionally, the maximum emission was not exactly at 475 nm, but rather shifted to a higher wavelength; fig 4.5 (b), (c), and (d). Based on our findings, we suggest that SDS molecules are binding onto the surface of the papain protein. This binding phenomenon can be attributed to the occurrence of electrostatic interactions between SDS and papain.

### SDS-induced hydrophobic changes of Papain: Papain concentration dependence

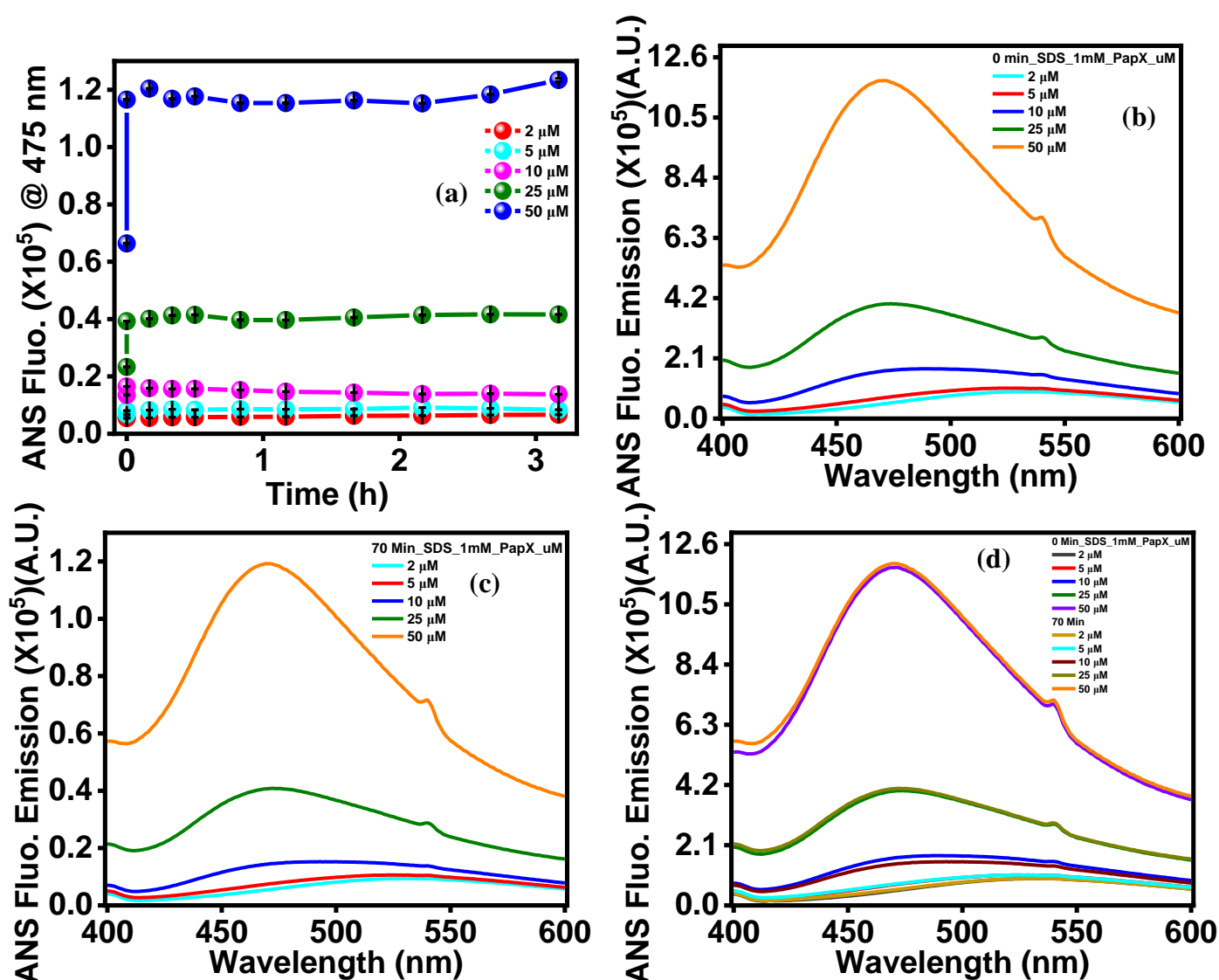


**Figure 4.7** (a) ANS fluorescence intensity at 475 nm as a function of time in absence and presence of 1 mM SDS, at varied papain concentration. (b) and (c) shows ANS fluorescence emission at 0 min and 70 min in the presence of 1 mM SDS, at varied protein concentration. (d) shows the combined plot at 0 min and 70 min.

Protein concentration dependent results showed an increase in the ANS fluorescence emission and the increment was directly proportional to the papain concentration and from the spectral graphs, we also observed a blue shift from ~525 nm to ~475 nm indicating that at lower concentration of papain the hydrophobic groups were hidden in the native protein while at higher concentration the hydrophobic part were getting exposed; fig 4.7 (b), (c), (d). This shows that the hydrophobicity plays an important role in the SDS- papain interaction.

#### **Charge on papain using SDS- inducer: SDS concentration dependent**

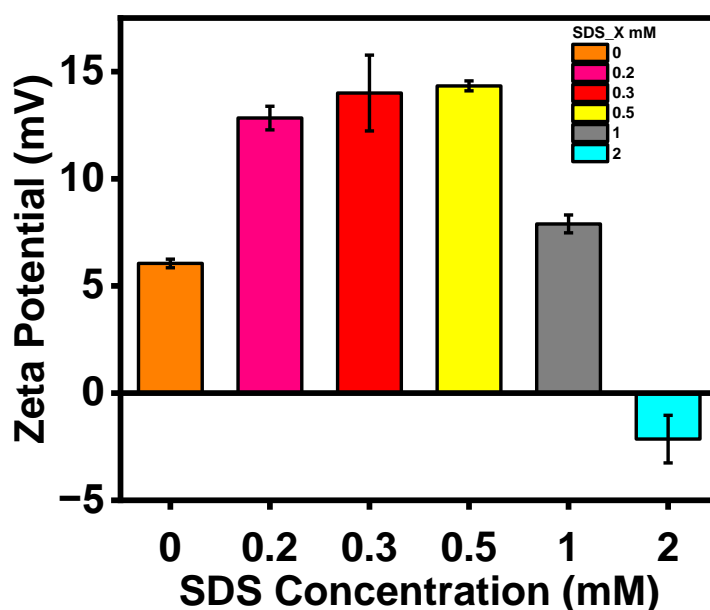


**Figure 4.8** Zeta potential measurements at 5  $\mu$ M papain, in absence and presence of variable SDS concentration.

To examine the charge on protein in the absence and presence of SDS we performed zeta potential measurement experiments. The pI of papain is ~9.02, as expected at pH 7.4, papain should have an overall positive charge, which was even confirmed with zeta potential measurements. At lower concentration of SDS the overall charge on protein was found to be positive and was increasing on increasing the SDS concentration upto 1 mM and on further increasing the SDS concentration to 2 mM, the overall charged on protein was found to be negative indicating surface charged neutralization. This may be due to the electrostatic attraction between the positively charged amino acid residues of protein and the negatively charged SDS.

### SDS-induced structural changes of Papain: SDS concentration dependence

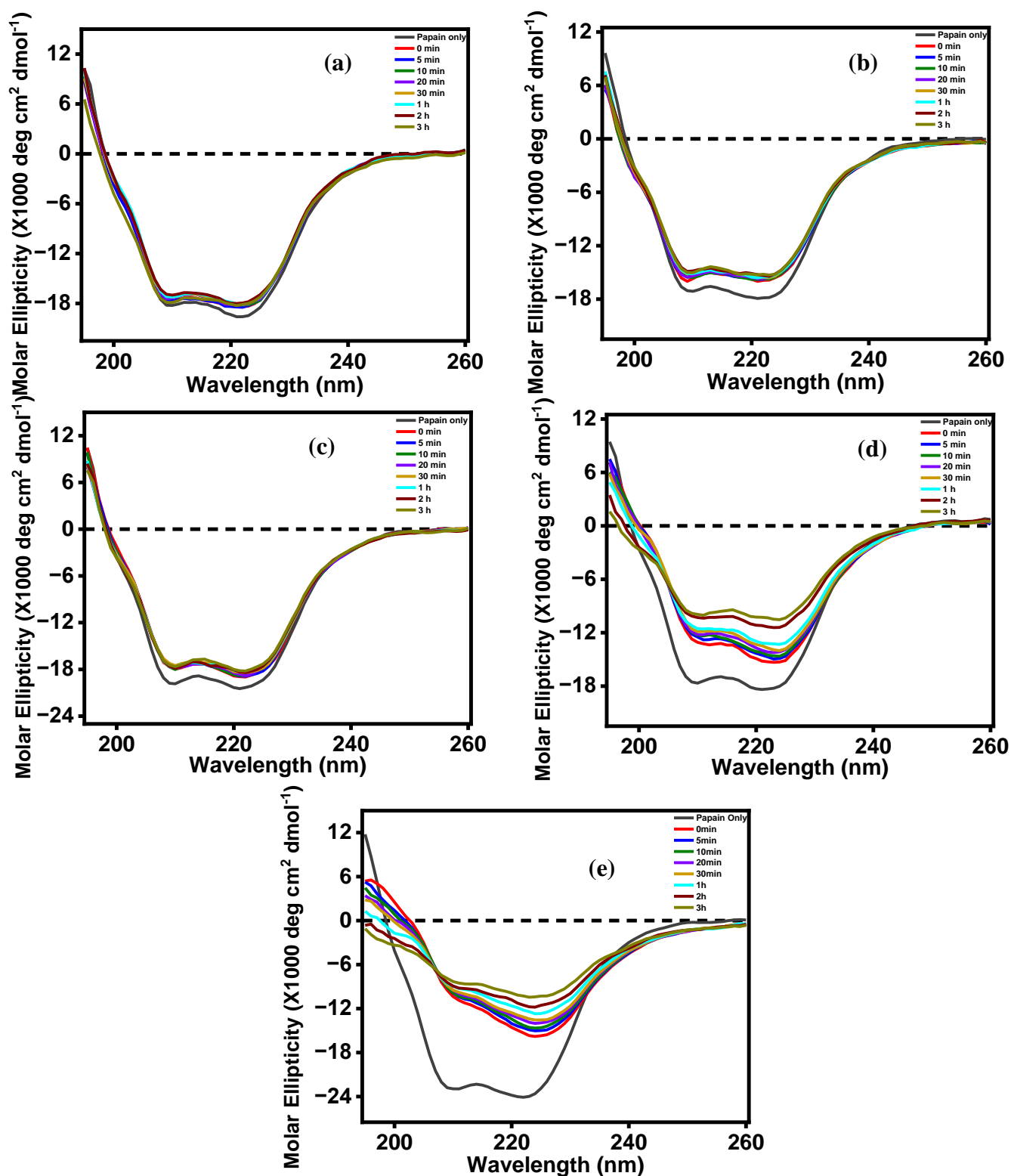


**Figure 4.9** Far UV-CD Spectra as a function of time at 5  $\mu\text{M}$  protein, in the absence and presence of varied SDS concentration. (a), (b), (c), (d) and (e) graphs shows the 200  $\mu\text{M}$ , 300  $\mu\text{M}$ , 500  $\mu\text{M}$ , 1 mM and 2 mM SDS concentrations.

We have further elucidated the secondary structural changes in papain during the course of aggregation by monitoring the changes in far-UV CD spectra. For these set of experiments, we have varied SDS concentration and keeping the papain concentration constant at 5  $\mu\text{M}$ . It is noteworthy that the presence of minima at 208 nm and 222 nm, a hallmark of  $\alpha$ -helical secondary structure, was a defining property of all the spectra. We observed a decrease in negative ellipticity at 208 nm and 222 nm indicative of loss in  $\alpha$ -helical content of the protein and the extent of decrease was found to be prominent with increasing SDS concentration. We have also deconvoluted the data and the results showed that, at 200  $\mu\text{M}$  SDS, there was no change in the secondary structural content; fig 4.9 (a). At 300  $\mu\text{M}$  SDS, we observed an increase in random coils at the expense of  $\alpha$ -helices but no change in the  $\beta$  content; fig 4.9 (b). But as we moved to higher concentration of SDS, we observed a significant increment in the  $\beta$ - content. Upon the addition of 500  $\mu\text{M}$  SDS, an increase in  $\beta$ - sheets was observed at the expense of  $\alpha$ -helices but no change in the random coils; fig 4.9 (c). Similarly, at 1 mM, there was a significant increase in  $\beta$ - sheets at the expense of  $\alpha$ -helices and no change in the random coils; fig 4.9 (d). For 2 mM SDS also, we observed an increase in both  $\beta$ - sheets and random coils at the expense of  $\alpha$ -helices but the extent of increment was more for  $\beta$ - sheet as compared to random coil; fig 4.9 (e). From above mentioned results we conclude that at lower SDS concentration ( $\leq 500 \mu\text{M}$ ), random coil were formed at the expense of  $\alpha$ -helices and no such change in the  $\beta$ - sheets was observed. And at higher SDS concentration ( $\geq 500 \mu\text{M}$ ),  $\beta$ -sheets were formed at an expense of  $\alpha$ - helices.

### **Rotational flexibility of Papain in the presence of SDS- inducer: SDS concentration dependence**

Steady-state fluorescence anisotropy gives an information regarding the rotational mobility of a fluorophore. Firstly, we recorded the steady-state tryptophan fluorescence anisotropy of 5  $\mu\text{M}$  papain in the presence of variable concentration of SDS as a function of time. In the presence of SDS, we observed an increase in the tryptophan fluorescence anisotropy and it depends upon the SDS concentration. Upto 500  $\mu\text{M}$  SDS, there is a small but measurable increase in anisotropy but we observed a significant increase with 1 mM and 2 mM SDS. With all the concentration of SDS, there is no change in anisotropy with time that means whatever changes may occurred at 0 h that was remained unchanged for 3 h; fig.4.10. This increase in tryptophan anisotropy in the presence of SDS suggested that as SDS concentration is increasing, the rotational flexibility of tryptophan is decreasing indicating the formation of large-sized aggregates.

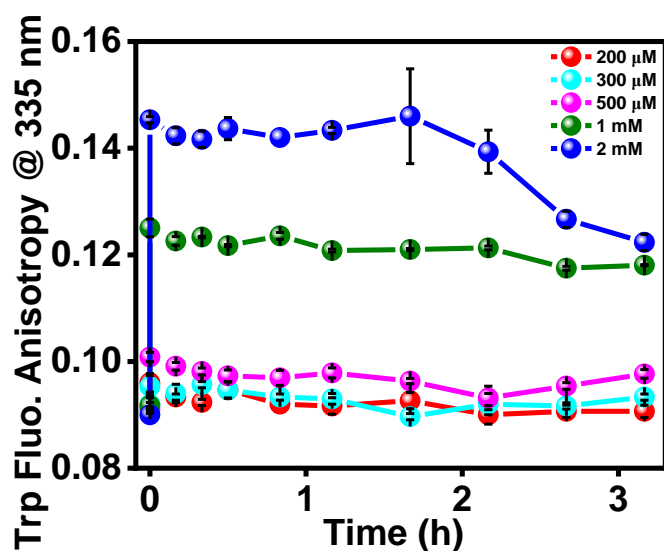


**Figure 4.10** Tryptophan fluorescence anisotropy monitored at 335 nm at 5  $\mu$ M papain, in absence and presence of variable SDS concentration.

**Rotational flexibility of Papain in the presence of SDS- inducer: Papain concentration dependence**

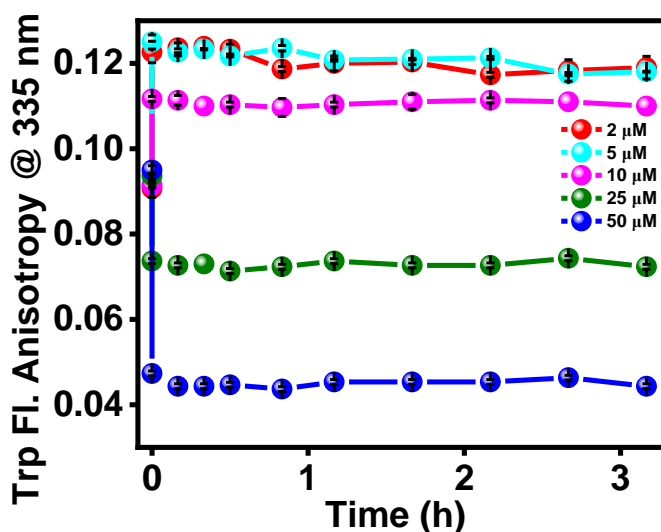


**Figure 4.11** Tryptophan fluorescence anisotropy monitored at 335 nm in absence and presence of 1 mM SDS, for variable papain concentration.

Similarly, the tryptophan fluorescence anisotropy was recorded in papain concentration dependent manner, keeping the SDS concentration constant to 1 mM. In the absence of SDS, no change in the tryptophan fluorescence anisotropy was observed but in the presence of SDS, the fluorescence anisotropy decreased with increase in papain concentration, in contrast to our expectation; fig 4.11. The probable reason for this decrement might be due to the

formation of large sized aggregates, that were settling down even upon mixing well. In conclusion, all the fluorescence experiments suggests that there was an enhancement in papain aggregation upon increasing the concentration of either papain or SDS or both.

### Morphological studies of aggregates using FESEM and TEM

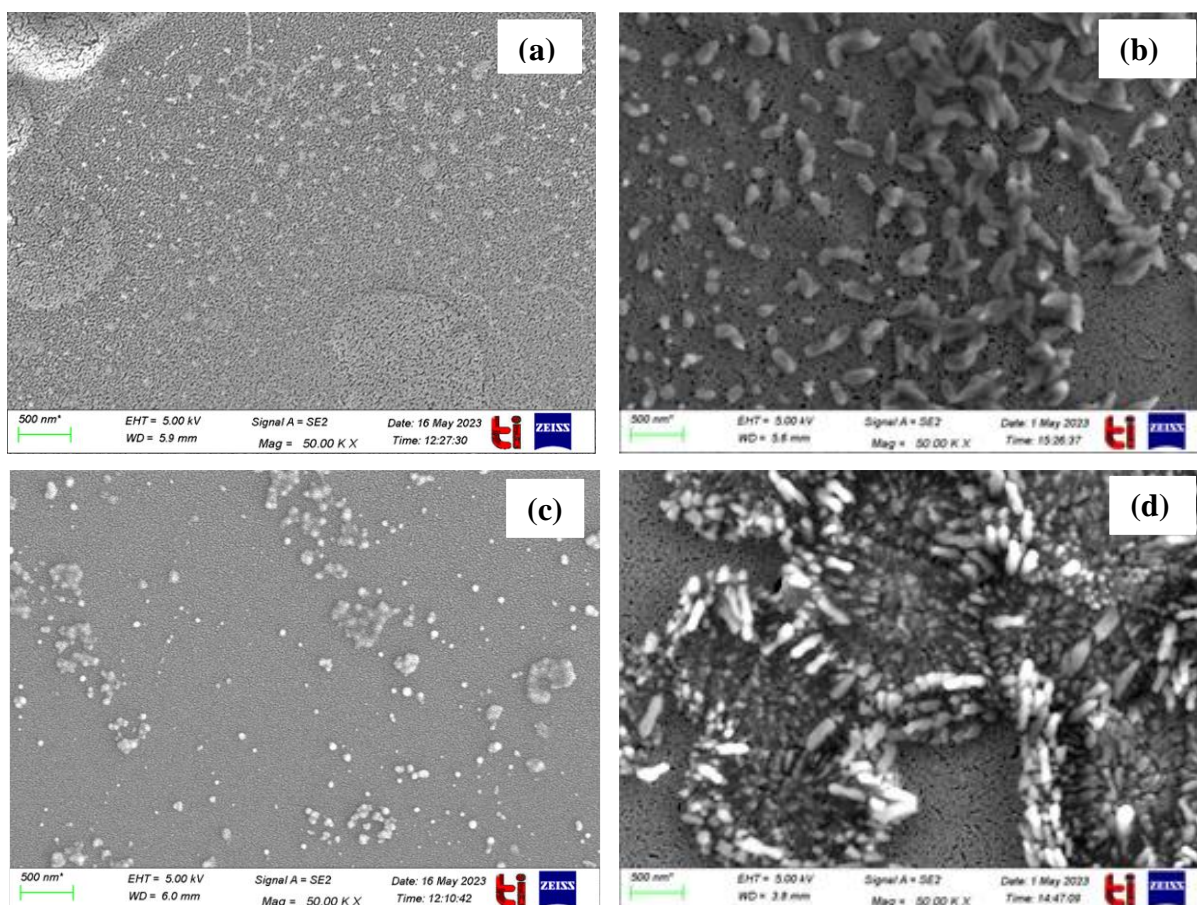


**Figure 4.12:** Field Emission- Scanning Electron Microscopy images representing the morphology of aggregates; (Scale: 500 nm). (a) papain [5  $\mu\text{M}$ ] and SDS [300  $\mu\text{M}$ ], (b) papain [5  $\mu\text{M}$ ] and SDS [1 mM] , (c) papain [5  $\mu\text{M}$ ] and SDS [2 mM], (d) papain [50  $\mu\text{M}$ ] and SDS [1 mM].

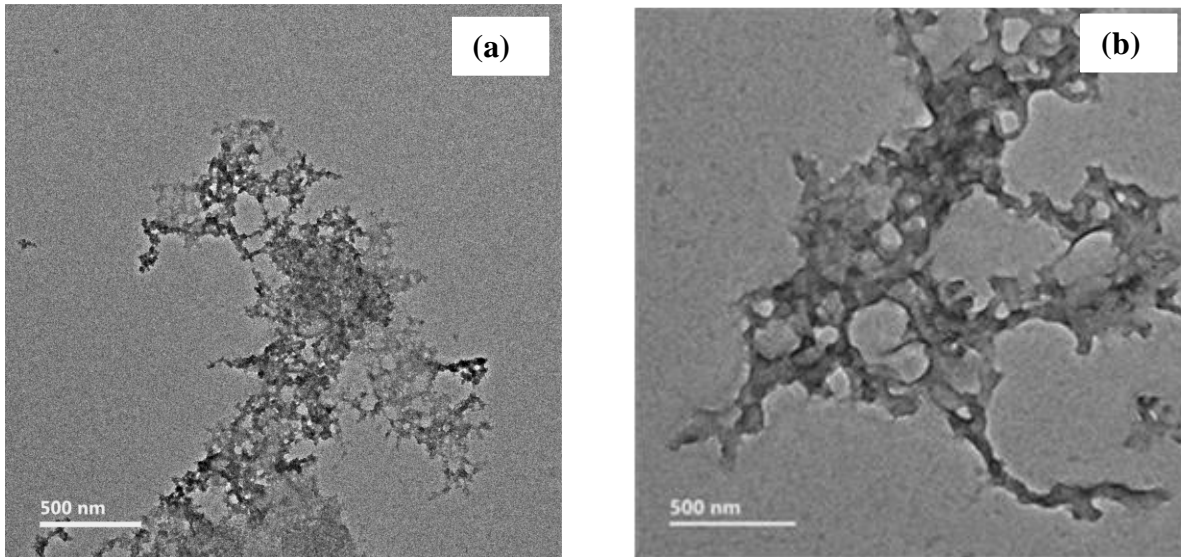


**Figure 4.13:** Transmission Electron Microscopy images representing the morphology of aggregates; (Scale: 500 nm). (a) papain [5  $\mu$ M] and SDS [1 mM] ,(b) papain [50  $\mu$ M] and SDS [1 mM].

We examined the morphology of aggregates under different conditions using FESEM and TEM microscopy techniques. The FESEM and TEM images further confirmed that the aggregates were amorphous in nature, not fibrillar. Also, we observed that with the increase in concentration of SDS and papain concentration remains constant, the formation of aggregation was increased ; fig. 4.12 (a), (b), (c) and fig. 4.13 (a). At higher concentration of papain, a large amount of aggregates were formed; fig 4.12 (d) and fig. 4.13 (b).

## **CONCLUSION**

We studied the aggregation of papain in the presence of SDS (anionic surfactant) at pH 7.4 and room temperature using various spectroscopic and microscopic techniques. The bioinformatic tools were useful to get insight into intrinsic characteristics of papain and get knowledge about the aggregation propensity of protein. We have obtained an enhancement in papain aggregation upon increasing the concentration of either SDS or papain or both, indicating that protein concentration as well as the concentration of a charged additive (specifically SDS in our study) has an influential role during papain aggregation. Morphological images using SEM further confirmed the amorphous nature of these aggregates. Also, far-UV CD experiments revealed a loss in secondary structural content of the protein. Based on our experiments, we concluded that there was an electrostatic interactions between negatively charged SDS and positively charged papain at pH 7.4 ( $\text{pH} < \text{pI}$ ). This exposes the hydrophobic region of papain resulting in hydrophobic interactions between protein and hydrophobic tail of SDS resulting into the aggregation of papain. Therefore, both electrostatic and hydrophobic interactions plays a crucial role during SDS-induced papain aggregation. In conclusion, protein structural and conformational stability is affected due to modulation in the electrostatic and hydrophobic interactions, leading to protein aggregation. Therefore, this work helps us to understand the important role of interactions during protein aggregation.

## **REFERENCES**

1. Stollar, E.J.; Smith, D.P. Uncovering protein structure. *Essays Biochem.* **2020**, *64*, 649- 680.
2. Pastore, A.; Martin, S.R.; Temusi, P.A. A generalized view of protein folding: In meto stat virtus. *J. Am. Chem. Soc.* **2018**, *141(6)*, 2194- 2200.
3. Lapidus, L.J. Protein unfolding mechanisms and their effects on folding experiments. *F1000 Res.* **2017**, *6*.
4. Buchner, G.S.; Murphy, R.O.; Buchete, N.V.; Kubelka, J. Dynamics of protein folding: Probing the kinetic network of folding- unfolding transitions with experiments and theory. *Biochem. Biophys. Acta* **2011**, *1814*, 1001- 1020.
5. Housmans, J.A.J.; Wu, G.; Schymkowitz, J.; Rousseau, F. A guide to studying the protein aggregation. *FEBS Journal* **2021**, *290*, 554- 583.
6. Wang, W.; Newa, S.; Teagarden, D. Protein aggregation- Pathways and influencing factors. *Int. J. Pharm.* **2010**, *390*, 89- 99.
7. Wang, W. Protein aggregation and its inhibition in biopharmaceutics. *Int. J. Pharm.* **2005**, *289*, 1-30.
8. Belton, D.J.; Miller, A.F. Thermal Aggregation and Recombinant Protective Antigen: Aggregate Morphology and Growth Rate. *J. Biophys.* **2013**.
9. Linding, R.; Schymkowitz, J.; Rousseau, F.; Diella, F.; Serrano, L. A comparative study of the Relationship between Protein Structure and  $\beta$ - Aggregation in Globular and Intrinsically Disordered Proteins. *J. Mol. Biol.* **2004**, *342*, 345- 353.
10. Khan, J.M.; Qadeer, A.; Chaturvedi, S.K.; Ahmad, E.; Rehman, S.A.A.; Gourinath, S.; Khan, R.H. SDS can be utilized as an Amyloid Inducer: A case study on diverse proteins. *PLoS ONE* **2012**, *7*.
11. Biancalana, M.; Koide, S. Molecular mechanism of Thioflavin-T binding to amyloid fibrils. *Biochim. Biophys. Acta* **2010**, *1804*, 1405- 1412.
12. Iadanza, M.G.; Jackson, M.P.; Hewitt, E.W.; Ranson, N.A.; Radford, S.E. A new era for understanding amyloid structure and disease. *Nat. Rev. Mol. Cell Biol.* **2018**, *19(12)*, 755-773.
13. Tacias- Pascacio, V.G.; Morellon-Sterling, R.; Casteneda-Valbuena, D.; Berenguer-Murcia, A.; Kamli, M.R.; Tavano, O.; Fernandez- Lafuente, R. Immobilization of papain. *Int. J. Biol. Macromol.* **2021**, *188*, 94-113.

14. Holyavka, M.; Pankova, S.; Koroleva, V.; Vyshkvorkina, V.; Lukin, A.; Kondratyev, M.; Artyukhov, V. Influence of UV radiation on molecular structure and catalytic activity of free and immobilized bromelain, ficin and papain. *J. Photochem. Photobiol. B.* **2019**, *201*, 116681.
15. Raskovic, B.; Popovic, M.; Ostojic, S.; Anelkovic, B.; Tesevic, V.; Polovic, N. Fourier transform infrared spectroscopy provides an evidence of papain denaturation and aggregation during cold storage. *Spectrochim. Acta A Mol. Biomol. Spectrosc.* **2015**, *150*, 238- 246.
16. Llerena- Suster, C.R.; Jose, C.; Collins, S.E.; Briand, L.E.; Morcelle, S.R. Investigation of the structure and proteolytic activity of papain in aqueous miscible organic media. *Process Biochem.* **2012**, *47*, 47- 56.
17. Sangeetha, K.; Abraham, T.E. Chemical modification of papain for use in alkaline medum. *J. Mol.Cat. B.* **2006**, *38*, 171- 177.
18. Saringer, S.; Akula, R.A.; Szerlauth, A.; Szilagyi. Papain adsorption on Latex Particles: Charging, Aggregation, and Enzymatic Activity. *J. Phys. Chem. B* **2019**, *123 (46)*, 9984-9991.
19. Huet, J.; Looze, Y.; Bartik, K.; Raussens, V.; Wintjens, R.; Boussard, P. Structural Characterization of the papaya cysteine proteinases at low pH. *Biochem. Biophys. Res. Commun.* **2006**, *341*, 620-626.
20. Kamphaus, I.G.; Kalk, K.H.; Swarte, M.B.A.; Drenth, J. Structure of Papain at 1.65 Å Resolution. *J. Mol. Biol.* **1984**, *179*, 233-256.
21. Stepek, G.; Behnke, J.M.; Buttle, D.J.; Duce, I.R. Natural plant cysteine proteinases as anthelmintics. *Trends Parasitol* **2004**, *20*, 322-7.
22. Edwin, F.; Jagannadham, M.V. Sequential unfolding of papain in molten globule state. *Biochem. Biophys. Res. Commun.* **1998**, *252*, 654-660.
23. Kimmel, J.R.; Smith E.L. Crystalline Papain. *J. Biol. Chem.* 1954, *207(2)*, 515-31.
24. Kuwajima, K. The molten globule state as a clue for understanding the folding and cooperativity of Globular Protein structure. *Alan R. Liss* **1989**, *6*, 87- 103.
25. Amri, E.; Mamboya, F. Papain- A plant enzyme of biological importance. *Am. J. Biochem. Biotech.* **2012**, *8 (2)*, 99- 104.
26. Chamani, J.; Heshmati, M.; Rajabi, O.; Parivar K. Thermodynamic study of Intermediate state of papain induced by n- alkyl sulfates at two different pH values: A spectroscopic approach. *SURF. Sci.* **2009**, 20-29.

27. Baker, E. N.; Drenth, J.; Kamphauis, I.G. Thiol Proteases comparative studies based on the High- resolution structures of Papain and Actinidin and on Amino Acid Sequence information for Cathepsins B and H and Stem Bromelain. *J. Mol. Biol.* **1985**, *182*(2), 317- 329.
28. Stevenson, D. E.; Storer, A.C. Papain in organic solvents: Determination of conditions suitable for Biocatalysis and the effect on substrate specificity and inhibition. *Biotechnol. Bioeng.* **1991**, *37*(6), 519- 527.
29. Fink, A.L.; Calciano, L. J.; Goto, Y.; Kurotsu, T.; Pulleros, D. R. Classification of Acid denaturation of Proteins: Intermediates and unfolded states. *Biochemistry* **1994**, *33*, 12504- 12511.
30. Edwin, F.; Sharma, Y.V.; Jagannadham, M.V. Stabilization of Molten Globule state of Papain by Urea. *Biochem. Biophys. Res. Commun.* **2002**, *290*(5), 1441- 1446.
31. Arano, A. M.; Garcia, M. S. Detection and characterization by circular dichroism of a stable intermediate state formed in the thermal unfolding of papain. *Biochim. Biophys. Acta* **1988**, *954*, 170- 175.
32. Qadeer, A.; Zaman, M.; Khan, R.H. The inhibitory effect of Post- Micellar SDS concentration on Thermal Aggregation and Activity of Papain. *Biochemistry (Moscow)* **2014**, *79*, 785- 796.
33. Chamani, J.; Heshati, M. Mechanism for stabilization of the molten globule state of papain by sodium n- alkyl sulfates: Spectroscopic and Calorimetric approaches. *J. Colloid Interface Sci.* **2008**, *322*, 119- 127.
34. Ghosh, S. Conformational study of papain in the presence of sodium dodecyl sulfate in aqueous medium. *Colloids Surf B Biointerfaces* **2005**, *41*, 209- 216.
35. Ghosh, S. Physicochemical and conformational studies of papain/ sodium dodecyl sulfate system in aqueous medium. *Colloids Surf A: Physicochem. Eng. Aspects* **2005**, *264*, 6- 16.
36. Naeem, A.; Fatima, S.; Khan, R.H. Characterization of partially folded intermediates of papain in the presence of Cationic, Anionic and Nonionic Detergents at low pH. *Biopolymers* **2006**, *83*(1), 1-10.
37. LaLonde, J.M.; Zhao, B.; Smith, W.W.; Janson, C.A.; DesJarlais, R.L.; Tomaaszek, T.A.; Carr, T.J.; Thompson, S.K.; Oh, H.J.; Yamashita, D.S.; Veber, D.F.; Abdel-Megyid, S.S. Use of Papain as a model for the structure-based design of Cathepsin K inhibitors: Crystal structure of Two Papain- Inhibitor Complexes Demonstrate Binding to S'- subsites. *J. Med. Chem.* **1998**, *41*, 4567-4576.

## Document Information

---

Analyzed document	Nitika_Thesis.docx (D172092429)
Submitted	2023-07-14 21:29:00
Submitted by	Dr. Mily Bhattacharya
Submitter email	mily.bhattacharya@thapar.edu
Similarity	0%
Analysis address	mily.bhattacharya.thapar@analysis.arkund.com

## Sources included in the report

---

### Entire Document

---

Spectroscopic investigation into papain conformational changes in the presence of an anionic surfactant  
A Dissertation Submitted for the partial fulfilment of the Degree of Master of Science In Chemistry By Nitika Aggarwal  
(Registration No.: 302102013)

Under the guidance of

Dr. Mily Bhattacharya (Assistant Professor)

School of Chemistry and Biochemistry Thapar Institute of Engineering and Technology Patiala - 147004, Punjab

#### CANDIDATE'S DECLARATION

I, hereby, declare that the work being presented in the dissertation entitled "Spectroscopic investigation into papain conformational changes in the presence of an anionic surfactant" in partial fulfilment of the requirement for the award of the degree of Masters of Science in Chemistry and being submitted to School of Chemistry and Biochemistry, Thapar Institute of Engineering and Technology, Patiala is my own research work carried out during the period of January to July 2023 under the supervision of Dr. Mily Bhattacharya. I have not submitted the contents embodied in this dissertation for the award of any degree elsewhere.

Nitika Aggarwal

Date:

It is certified that the above statement made by the student is correct to the best of my knowledge and belief.

Dr. Mily Bhattacharya Assistant Professor School of Chemistry and Biochemistry Thapar Institute of Engineering and Technology, Patiala- 147004

CERTIFICATE This is to certify that the dissertation entitled "Spectroscopic investigation into papain conformational changes in the presence of an anionic surfactant", being submitted by Ms. Nitika Aggarwal in the partial fulfilment of requirement for the award of the degree of Masters of Science in Chemistry and being submitted to the School of Chemistry and Biochemistry, Thapar Institute of Engineering and Technology, Patiala is a bonafide work carried out by her under my supervision. The work has reached the standard necessary for submission, and the contents of this dissertation have not been submitted to any other university or institute for the award of any degree or diploma.

Dr. Mily Bhattacharya Assistant Professor School of Chemistry and Biochemistry Thapar Institute of Engineering and Technology, Patiala- 147004

